# The effect of redox probe solution composition on the response of the electrochemical biosensor

Bachelor's thesis

Student: David Tsaregorodtsev

Supervisor: Jekaterina Reut, Senior Lecturer

Department of Materials and Environmental Technology

Study programm: LAAB17/17

Tallinn 2022

# Redokspaari lahuse koostise mõju elektrokeemilise biosensori signaalile

Bakalaureusetöö

Üliõpilane: David Tsaregorodtsev

Juhendaja: Jekaterina Reut, vanemlektor

Materjali- ja keskkonnatehnoloogia instituut

Õppekava: LAAB17/17

Tallinn 2022

# Author’s declaration of originality

Hereby I declare that I have compiled the paper independently and all works, important standpoints and data by other authors have been properly referenced and the same paper has not previously been presented for grading.

Author: David Tsaregorodtsev

02.06.2022

The paper conforms to requirements in force.
Supervisor: Jekaterina Reut
[Signature, date]

Permitted to the defence.
Chairman of the Defence Committee: Vello Tõugu
[Signature, date]

# Abstract

## The effect of redox probe solution composition on the response of the electrochemical biosensor

The thesis deals with the optimization of a redox probe solution for an electrochemical biosensor, namely, a molecularly imprinted polymer (MIP)-based electrochemical biosensor. The topic is related to several research fields including electrochemistry, biosensors, and molecular imprinting technology. The study was carried out in the Laboratory of Biofunctional Materials at the Department of Materials and Environmental Technology of TalTech.

Biosensors are analytical devices incorporating a biological receptor (antibody, peptide, enzyme etc) interfaced with a physicochemical transducer to deliver complex bioanalytical measurements with simple, easy-to-use formats. The synthetic receptors prepared by molecular imprinting technology, the so-called MIPs, have been extensively studied as a more robust and inexpensive alternative to the labile biological receptors. The research group of the Laboratory of Biofunctional Materials has developed a MIP-based electrochemical biosensor, where an external redox probe solution containing 4mM of potassium ferri/ferrocyanide $K_3[Fe(CN)_6]/K_4[Fe(CN)_6]$ in 1M potassium chloride (KCl) was used to generate the sensor signal. Although the high supporting electrolyte concentration (1M KCl) is necessary to increase the solution conductivity and achieve the charge balance at the electrode/solution interface, it can adversely affect the structure of protein and consequently the sensor response. Therefore, an optimization of the redox probe solution is necessary to obtain the redox probe solution with the reduced concentration of KCl while not significantly affecting the MIP biosensor electrochemical response.

The aim of the thesis is to study the effect of the redox probe solution composition on the MIP-based electrochemical biosensor response to find the optimal solution composition. Cyclic voltammetry (CV) and differential pulse voltammetry (DPV) electroanalytical techniques were used to perform the electrochemical measurements. First, the electrochemical behavior of the redox probe solution of different concentrations of KCl and $[Fe(CN)_6]^{3-/4-}$ redox pair at the gold disc electrode was studied, aiming to identify a solution composition with a reduced concentration of KCl. Then, the selected redox probe solution was used to study the adsorption of a model protein (bovine serum albumin, BSA) on the gold electrode. Finally, the optimized redox probe was used to study the protein rebinding to the MIP-modified gold electrode or, in the other words, MIP-based biosensor. Based on the experimental results the solution containing 12 mM of $K_3[Fe(CN)_6]/K_4[Fe(CN)_6]$ in 0.3 M KCl was selected as an optimal redox probe solution and was shown to be suitable for analyzing the response of the MIP-based biosensor. Due to the decreased salt concentration, the optimized probe solution is expected to be less affecting the native conformation of protein during the measurement procedure than the previous probe solution. It was demonstrated that the measurements in the optimized solution allowed to improve the sensor response at the low concentrations of target protein (BSA). The data and results collected and analyzed in this study can be used for future research aiming to improve the electrochemical readout of the MIP-based biosensor.

# Annotatsioon
# Redokspaari lahuse koostise mõju elektrokeemilise biosensori signaalile

Lõputöö eesmärgiks on redokspaari lahuse optimeerimine molekulaarselt jäljendatud polümeeri (MIP)-baasil elektrokeemilisele biosensorile. Teema on interdistsiplinaarne ja seotud elektrokeemia, biosensorite ja molekulaarse jäljendamise tehnoloogiaga. Uurimistöö on teostatud Tallinna Tehnikaülikooli Materjali- ja keskkonnatehnoloogia instituudi Biofunktsionaalse Materjalide laboratooriumis.

Biosensorid on analüütilised seadmed, kus bioloogiline tundlik element (antikeha, peptiid, ensüüm jne), on ühildatud muunduriga, mis muudab bioloogilise reaktsiooni mõõdetavaks elektriliseks signaaliks. Biosensorid võimaldavad kiiret, suure tundlikkusega ja selektiivsusega usaldusväärset analüüsi ning on tänapäeval leidnud laia kasutuse meditsiinis, keskkonnaseisundi jälgimisel ja teistes valdkondades. Biosensorite arendamisel on siiski veel probleemiks bioloogiliste retseptorite ebastabiilsus ja kallis hind. Üheks võimalikuks lahenduseks on bioloogiliste retseptorite asendamine sünteetiliste analoogidega, milleks sobivad näiteks molekulaarselt jäljendatud polümeerid (MIP). Oluliselt stabiilsemate omadustega MIP-d on võimelised sama efektiivselt siduma sihtmolekule nagu bioloogilised retseptorid. Biofunktsionaalse materjalide uurimisrühm töötas välja MIP-baasil elektrokeemilise biosensori. Sensori tööpõhimete seisneb välise redokspaari elektrokeemilisest reaktsioonist tingitud voolutugevuse intensiivsuse kahanemise mõõtmisele sensorkiibi ja lahuse piirpinnal peale sihtmolekulide seostumist MIP-il. Kahanemise määr korreleerub viirusvalgu kontsentratsiooniga proovis. Kasutatud välise redokspaari lahus koosnes 4mM kaaliumferri/ferrotsüaniidist $K_3[Fe(CN)_6]/K_4[Fe(CN)_6]$ ja 1M kaaliumkloriidist (KCl). Kuigi kõrge elektrolüüdi kontsentratsioon (1M KCl) on vajalik lahuse juhtivuse suurendamiseks ja laengute tasakaalu saavutamiseks elektroodi/lahuse piirpinnal, võib see siiski mõjutada analüüsitava valgu struktuuri ja sellest tulenevalt ka sensori signaali. Seetõttu on vaja kohandada redokspaari lahuse koostist nii, et KCl kontsentratsiooni vähendamine ei mõjutaks olulisel MIP-baasil biosensori elektrokeemilist signaali.

Lõputöö eesmärgiks oli uurida, kuidas redokspaari lahuse koostis mõjub MIP elektrokeemilise biosensori signaalile ja leida optimaalne lahuse koostis. Elektrokeemilised mõõtmised viidi läbi tsüklilise voltamperomeetria (CV) ja differentsiaalse impulss voltamperomeetria (DPV) abil. Esialgselt, uuriti redokspaari lahuse elektrokeemilist käitumist erinevate elektrolüüdi KCl ja redokspaari $[Fe(CN)_6]^{3-/4-}$ kontsentratsioonidega lahustes puhtal kuldelektroodil, eesmärgiga leida sobiv vähendatud KCl kontsentratsiooniga lahus. Seejärel kasutati leitud redokspaari lahust mudelvalgu (veise seerumi albumiin, BSA) adsorptsiooni uurimiseks puhtal kuldelektroodil. Lõpuks kasutati optimeeritud redokspaari lahust BSA spetsiifilise sidumise uurimiseks MIP-ga modifitseeritud kuldelektroodil ehk MIP-põhisel biosensoril. Katsetulemustest selgus, et lahus koostisega 12mM $K_3[Fe(CN)_6]/K_4[Fe(CN)_6]$ ja 0.3M KCl on sobiv biosensori uurimiseks. Kuna KCl kontsentratsioon on madalam võrreldes varem kasutatud lahusega, on lootust, et optimeeritud redokspaari lahus mõjutab elektrokeemilistel mõõtmistel valgu struktuuri vähem. Töös näidati, et mõõtmised optimeeritud kontsentratsiooniga lahuses võimaldasid parandada MIP biosensori signaali uuritava valgu (BSA) madalate kontsentratsioonide korral. Lõputöös kogutud ja analüüsitud andmeid ja tulemusi saab kasutada tulevastes uuringutes MIP-põhise biosensori elektrokeemilise signaali parandamiseks.

# List of abbreviations and terms

| | |
|---|---|
| AA | Acetic Acid |
| Ag/AgCl/$KCl_{sat}$ | Silver/Silver Chloride/Saturated KCl Electrode |
| 4-ATP | 4-Aminothiophenol |
| BSA | Bovine Serum Albumin |
| CE | Counter Electrode |
| CV | Cyclic Voltammetry |
| DPV | Differential Pulse Voltammetry |
| DTSSP | 3,3′-Dithiobis[sulfosuccinimidylpropionate] |
| 2-ME | 2-Mercaptoethanol |
| MIP | Molecular Imprinted Polymers |
| mPD | meta-Phenylenediamine |
| MQ | Millipore(ultrapure) Water |
| NIP | Non Imprinted Polymers |
| PBS | Phosphate-buffered saline |
| PmPD | Poly(m-phenylenediamine) |
| RE | Reference Electrode |
| TPS | Traditional Probe Solution |
| UPS | Upgraded Probe Solution |
| WE | Working Electrode |

# Table of contents

# Introduction

Biosensors are analytical devices incorporating a biological sensing element (receptor) interfaced with a physicochemical transducer to deliver complex bioanalytical measurements with simple, easy-to-use formats. The biosensing devices combine high selectivity of biomolecular recognition and sensitivity of modern signal-detection technologies offering a promising and powerful analytical tool in environmental monitoring[1], medical diagnostics[2], and many other fields. However, despite the significant progress in biosensors development, there is a significant limitation mainly associated with their labile nature, environmental instability as well as costly and time-consuming production[3]. Inspired by nature, researchers have created their own method to produce biomimetic materials recognizing molecules according to the same principle as biological receptors, i.e. the "lock and key" principle and called it the method of molecular imprinting[4]. The technique allows the formation of specific recognition sites in synthetic polymers using templates or imprint molecules resulting in so-called ”molecularly imprinting polymers” or MIPs. MIPs have been considered as inexpensive and robust alternatives for biorecognition elements of biosensors[5]. MIP-based sensors have been widely investigated as promising analytical devices in the field of medical diagnostics aiming the detection of very diverse analytes as biomarkers for early detection of diseases ranging from small molecules[6], to proteins and other biomacromolecules[7], Particularly, MIP-based electrochemical sensors can be considered advantageous due to the simplicity and low cost of the electrochemical transducer, e.g. screen-printed-electrode, as well as the possibility of fast measurement and compatibility with point-of-care testing[8]. Recently, the research group of the Laboratory of Biofunctional Materials at TalTech has developed a MIP-based electrochemical sensor for detection of SARS-CoV-2 viral protein, e.g. nucleocapsid and spike proteins[9,10]. Since the analyte (protein) is a non-electroactive molecule, an external redox probe solution containing 4mM of potassium ferri/ferrocyanide $K_3[Fe(CN)_6]/K_4[Fe(CN)_6]$ in 1M potassium chloride (KCl) was used to generate the sensor signal. This indirect electrochemical readout depended on the diffusional permeability of the MIP layer to the ferri/ferrocyanide ions, so-called “gate-effect”[11]. Nevertheless, the high concentration of electrolyte can adversely affect the structure of protein and consequently the sensor response[12]. On the other hand, the high supporting electrolyte concentration is necessary to increase the solution conductivity and achieve the charge balance at the electrode/solution interface as well as to prevent charged electroactive species from migrating in the electric field gradient[13]. Therefore, simple reduction of the KCl concentration seems to be not a good choice since it can seriously affect the electrochemical signal of the sensor. An optimization of the redox probe solution is necessary to obtain the redox probe solution with the reduced concentration of KCl while possessing the similar electrochemical behavior as the commonly used probe solution and not significantly affecting the MIP biosensor electrochemical response.

The aim of the thesis was to study the effect of the redox probe solution composition on the MIP-based electrochemical biosensor response to find the optimal solution composition. First, the electrochemical behavior of the redox probe solution of different concentrations of KCl and $[Fe(CN)_6]^{3-/4-}$ redox pair at the gold disc electrode was studied, aiming to identify a solution composition with a reduced concentration of KCl. Then, the selected redox probe solution was used to study the adsorption of a model protein (bovine serum albumin, BSA) on the bare gold electrode. Finally, the optimized redox probe was used to study the protein rebinding to the MIP-modified gold electrode or, in the other words, MIP-based biosensor. Cyclic voltammetry (CV) and differential pulse voltammetry (DPV) electroanalytical techniques were used to perform the electrochemical measurements. Based on the experimental results the solution containing 12 mM of $K_3[Fe(CN)_6]/K_4[Fe(CN)_6]$ in 0.3 M KCl was selected as an optimal

redox probe solution and was shown to be suitable for analyzing the response of the MIP-based biosensor. Due to the decreased salt concentration, the optimized probe solution is expected to be less affecting the native conformation of protein during the measurement procedure than the previous probe solution. It was demonstrated that the measurements in the optimized solution allowed to improve the sensor response at the low concentrations of target protein (BSA).

# 1. Literature Review

## 1.1. Basics of electrochemistry

Electricity is the set of physical phenomena associated with the presence and motion of matter that has a property of electric charge. The term «electricity» was introduced by British scientist William Gilbert in his thesis «*On the Magnet and Magnetic Bodies, and on the Great Magnet the Earth*»[14], where he described magnetic properties in the working principles of compasses. The simplified scheme of the generation of electricity - the flow of electric charge - in an electronic conductor is shown in Figure 1.

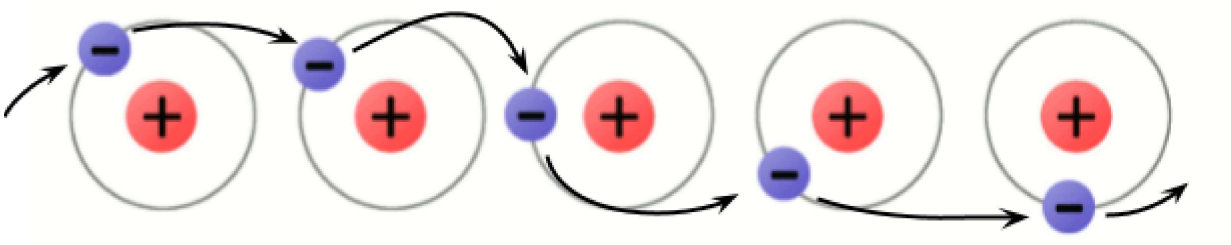

*Figure 1. Simplify model of charges flowing through atoms to make current (adapted from [15]).*

Electrochemistry is the study of electricity and how it relates to chemical reactions. Namely, electricity can be generated by movements of electrons from one species to another in a reaction known as oxidation-reduction or redox reaction. In electrochemistry, the redox reaction occurs at the interface between an electrode and an electrolyte. Electrolytes are chemical substances (bases, acids and salts) that due to the dissociation in the solution provide charged ions: cations (positively charged) and anions (negatively charged), capable of producing current if the potential is applied. When charged particles diffuse to the electrode/electrolyte interface, the charge transfer takes place, namely, the processes of oxidation or reduction. This step is called the charge transfer reaction. Chemical species directly involved in the charge transfer reaction are called electroactive. They are in reduced (Red) form or oxidized (Ox) form and together can be formed into a redox pair. The redox reaction can be written as follows:

$$Ox + ze^{-} \leftrightarrow Red,$$

where $ze^-$ is the number of electrons in the electrode reaction.

If the oxidized and reduced species involved in an electrode reaction are in equilibrium at the electrode surface (a reversible reaction),the electrode potential is calculated using the Nernst equation:

$$E = E^0 - \frac{RT}{zF} ln \frac{a_{red}}{a_{ox}},$$

where $E^0$ - standard potential, V
$R$ - universal gas constant, 8,314 J/(K mol)
$T$ - temperature, K
$F$ - Faraday constant, 96485 C/mol
$z$ - number of electrons in the electrode reaction

$a_{red}$ -activity of the reduced form
$a_{ox}$ -activity of the oxidized form

To investigate redox reactions, electrochemical cells are commonly used in electrochemistry.

### 1.1.1. Electrochemical Cells

An electrochemical cell is a device to generate electrical energy from the spontaneous chemical reactions occurring in it, or use the electrical energy supplied to it to facilitate a chemical reaction that is not spontaneous. The first type of cell is called a galvanic cell, the second type is an electrolytic cell.

A galvanic cell, named after Luigi Galvani[16], who was the first to discover an "animal electricity", consists of two metal electrodes, each immersed in a separate glass filled with electrolyte solutions and connected by a salt bridge (Figure 2). The electrodes, called the anode and cathode, are connected by an external circuit. The salt bridge completes the circuit by allowing the flow of ions between the electrolytic solutions containing the electrodes as well as reduces the diffusion potential that occurs at the boundary of the separation of two solutions containing ions with different mobility. Thus, the salt bridge tube is usually filled with KCl since the ionic mobilities of $K^+$ and $Cl^-$ ions are similar.

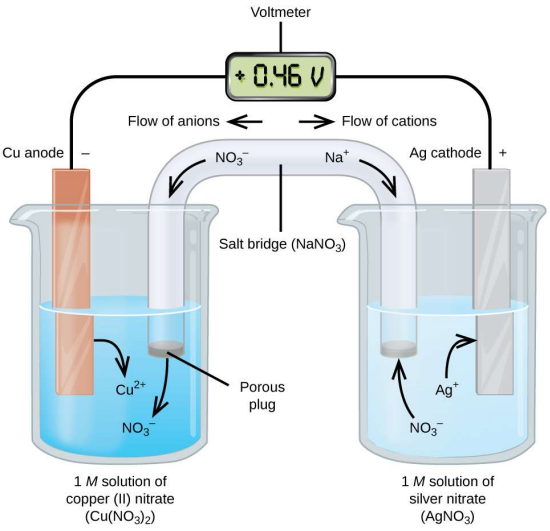


*Figure 2. Galvanic cell with Cu as anode and Ag as cathode*[17].

In the galvanic cell, electromotive force is a major characteristic parameter equal to the difference of catodic ($E_c$) and ($E_a$) potentials:

$$E = E_c - E_a$$

In an electrolytic cell, however, the opposite process, called electrolysis, occurs: an external voltage is applied to the electrode that pushes electrons through a chemical cell to drive a nonspontaneous reaction. These cells are employed in commercial processes such as electrolytic syntheses (e.g., the production of chlorine and aluminum), electrorefining (e.g., copper), and electroplating (e.g., silver and gold). In addition, they are frequently used in electroanalysis to conduct the voltammetric measurements[13]. A typical electrolytic cell for voltammetry has one reaction chamber, which contains

the electrolyte solution and along with the cathode and anode also include a reference electrode (RE) to control the potential in the cell (Figure 3). The quantitative aspects of electrolysis are described by Faraday's law, which determines the quantitative balance between the yield of the electrode reaction in terms of substance and the charge (Q) that has passed through the electrode:

$$m = kQ,$$

where *m* - mass of the substance is deposited on the electrode(g), *k* - electrochemical equivalent(g/C). The total charge, Q, is given by:

$$Q = It,$$

where *I* is the current (A) and t is the time (s).

The electric current generated by the redox reaction at the electrode and governed by Faraday's law is called faradaic current[13]. A faradaic current due to the analyte's reduction at the working electrode is a cathodic current, and an anodic current results from the analyte's oxidation. The faradaic current depends on the kinetics of electron transport and the rate at which redox particles diffuse to the electrode surface. Thus, for the ferri/ferrocyanide $[Fe(CN)_6]^{3-/4-}$ redox pair that is widely used as a standard probe in electrochemistry, the electron transfer kinetics is fast enough compared to the rate of the mass-transfer processes. The $[Fe(CN)_6]^{3-}$ reduction reaction:

$$Fe^{III}(CN)_6^{3-} + e- \rightarrow Fe^{II}(CN)_6^{4-}$$

Under this condition the surface concentrations of $[Fe(CN)_6]^{3-}$ and $[Fe(CN)_6]^{4-}$ are related to the electrode potential by the Nernst equation:

$$E = E^{0'} - \frac{RT}{zF} log \frac{[Fe(CN)_6^{4-}]}{[Fe(CN)_6^{3-}]}$$

where E is the applied potential and $E^{0'}$ is the formal electrode potential. It can be seen that as the applied potential becomes more negative the concentration of $Fe(CN)_6^{3-}$ must decrease at the electrode surface. It is being reduced to $Fe(CN)_6^{4-}$. At the same time their concentrations in bulk solution remain unchanged. Because of this difference in concentration, there is a concentration gradient between the solution at the electrode's surface and the bulk solution. This concentration gradient creates a driving force that transports $Fe(CN)_6^{4-}$ away from the electrode and that transports $Fe(CN)_6^{3-}$ to the electrode. This mass transport due the concentration gradient is called diffusion. The other mass transport modes in electrochemistry are migration and convection. Migration is due to the movement of charged particles in response to a local electric field. Migration can be eliminated by adding a high concentration of an inert supporting electrolyte. Convection occurs when the movement of the solution species is forced by mechanical stirring [18,19].

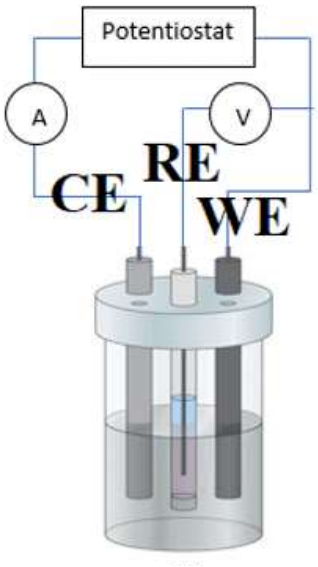


*Figure 3. Scheme of a three-electrode electrolytic cell, where , WE - working electrode, CE - counter electrode, RE - reference electrode (adapted from [20]).*

## 1.2. Electroanalytical techniques

Nowadays, electroanalytical methods, i.e. the electrochemical measurements for analytical purposes, have found a vast range of applications, including environmental monitoring, industrial quality control, and biomedical analysis[21]. The two principal types of electroanalytical measurements are potentiometry (the difference in electrode potentials is measured at zero current condition) and voltammetry (the cell's current is measured while actively altering the cell's potential). They have unique features such as sensitivity, selectivity, rapid response, requirement of low volume of solutions and easy usage[22]. In this thesis, two voltammetric methods: cyclic voltammetry (CV) and differential pulse voltammetry (DPV), were used for the electrochemical measurements.

### 1.2.1. Cyclic Voltammetry

CV is the most widely used technique for acquiring qualitative information about electrochemical reactions. It is capable of rapidly providing considerable information on the thermodynamics of redox processes, on the kinetics of heterogeneous electron-transfer reactions, and on coupled chemical reactions or adsorption processes. CV is often the first experiment performed in an electroanalytical study offering a rapid location of redox potentials of the electroactive species, and convenient evaluation of the effect of media on the redox process[21]. CV is generally used to study the redox reactions of a component in solution or of a molecule that is adsorbed onto the electrode. Although it was first practiced at hanging mercury drop electrodes (polarography)[23], it gained widespread use when solid electrodes like Pt, Au and carbonaceous electrodes were used, particularly to study anodic oxidations. CV consists of scanning linearly the potential of a working electrode using a triangular potential waveform (Fig. 4). The applied potential varies linearly with time between the initial starting value ($E_i$) and the final value of the forward scan ($E_{v1}$).During the potential scan, the current at the working electrode is plotted versus the applied potential difference to give a cyclic voltammogram(Fig. 5).

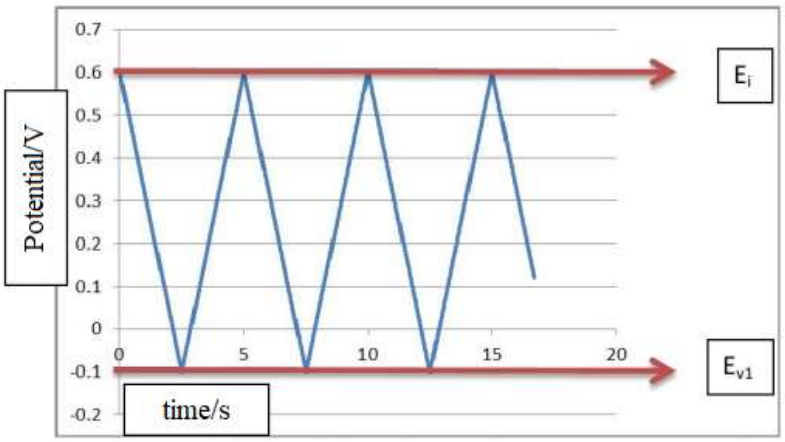


*Figure 4. Triangular potential-excitation signal for CV (adapted from [24]).*

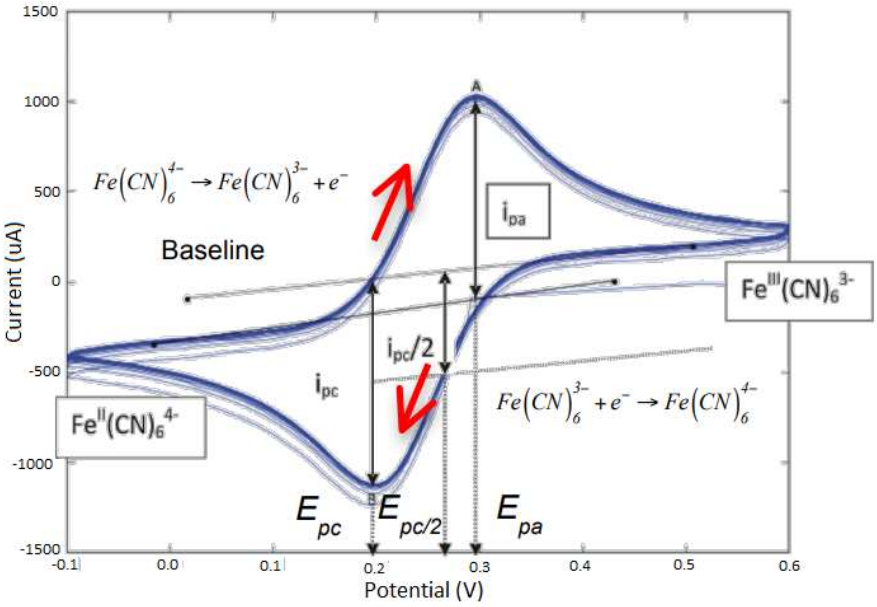


*Figure 5. A typical voltammogram for a reversible redox pair $[Fe(CN)_6]^{3-/4-}$ [24].*

The important parameters of a cyclic voltammogram are: the potential of the cathodic ($E_c$) and anodic ($E_a$) peaks and their difference ($\Delta E$), the intensity of the cathodic ($ip_c$) and anodic ($ip_a$) current peak.

The separation between the peak potentials ($\Delta E$) for a reversible couple is given by:

$$\Delta E = E_a - E_c = \frac{0{,}059}{n}$$

The peak separation can be used to determine the number of electrons transferred, and as criteria for the Nernst equation. A fast one-electron process exhibits a $\Delta E$ of about 0.059 V. But both the cathodic and anodic peak potentials are independent of the scan rate. And it is possible to relate the half-peak potential ($E_{p1/2}$) to the half-wave potential ($E_{1/2}$)[21]:

$$\Delta E_{p1/2} = E_{1/2} \pm \frac{0{,}028}{n}$$

The half-wave potential for a reversible process is very close to the value of the formal potential, $E^{0'}$ The formal potential for a reversible couple is centered between $E_{p,a}$ and $E_{p,c}$[21]:

$$E^{0'} = \frac{E_{p,a} + E_{p,c}}{2}$$

The current peak ($i_p$) of a reversible couple is described by the Randles-Sevick equation:

$$i_p = (2,69 * 10^5) Acn\sqrt{vD},$$

where *n* is the number of electrons, *A* is the electrode area($cm^2$), *c* is the concentration ($mol/cm^3$), *D* is the diffusion coefficient ($cm^2/s$), *v* is the scan rate (V/s). Accordingly, the current is directly proportional to concentration and increases with the square root of the scan rate. The ratio of the reverse-to-forward peak currents, $ip_a/ip_c$, is unity for a simple reversible couple. This peak ratio can be strongly affected by chemical reactions coupled to the redox process. The current peaks are commonly measured by extrapolating the preceding baseline current[21].

### 1.2.2. Differential Pulse Voltammetry

DPV is an extremely useful technique for measuring trace levels of organic and inorganic species. Pulse voltammetric techniques allow the lowering of the detection limit of measurements by substantially increasing the ratio between faradaic and non-faradaic (capacitive) currents[21]. The potential waveform for DPV is shown in Figure 6. The potential waveform consists of small pulses (of constant amplitude) superimposed upon a staircase waveform. Unlike normal pulse voltammetry, the current is sampled twice in each pulse period (once before the pulse, and at the end of the pulse), and the difference between these two current values is recorded and displayed. At the redox potential, the difference current reaches a maximum, and decreases to zero as the current becomes controlled by diffusion. The current response is therefore a symmetric peak as shown in Figure 7[25].

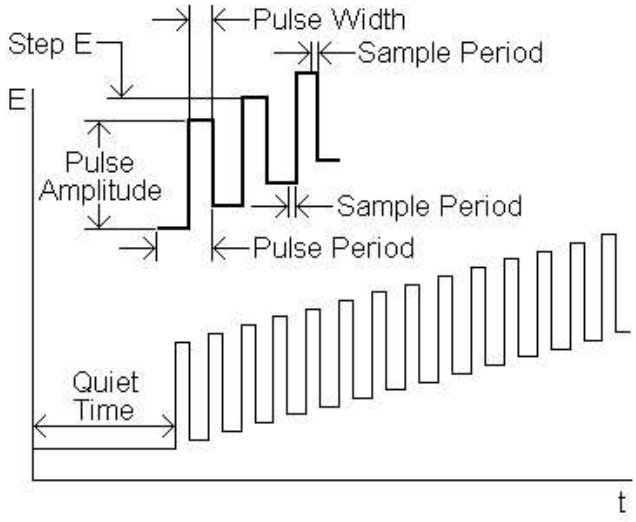


*Figure 6. Potential waveform for DPV*[25].

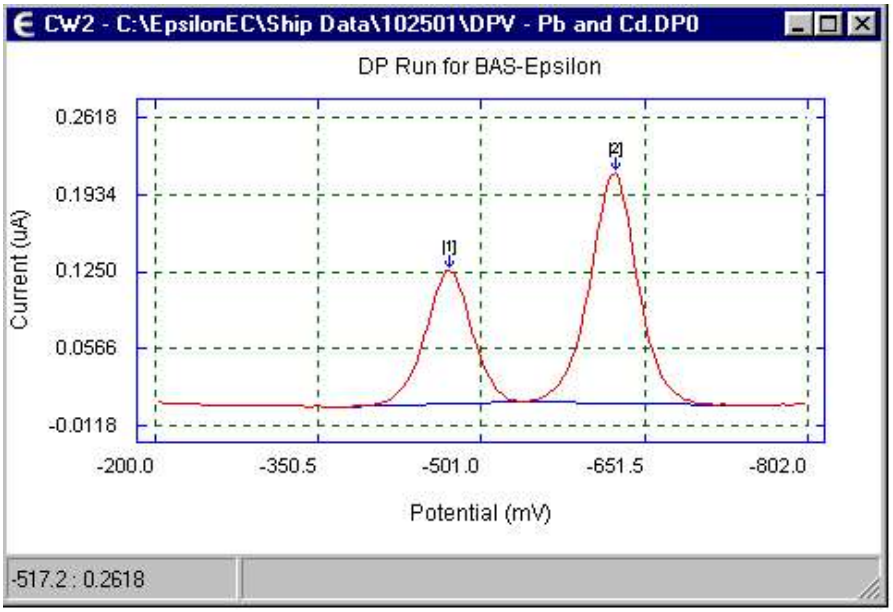


*Figure 7. A typical DPV plot*[25].

## 1.3. Biosensors and their types

Biosensors are analytical devices capable of detecting the specific molecule by a physico-chemical detector interfaced with a biorecognition element, usually a layer of biological receptors such as antibodies, enzymes, peptides etc. Biosensing principle is based on high specific intermolecular interactions such as antigen-antibody, ligand-receptor and complementarity of genetic molecules[26]. Biosensors are traditional tools of drug discovery, medical diagnostics, safety and security[3]. The best-known example of a biosensor is the blood glucose analyzer, which uses the glucose oxidase enzyme that catalyzes the oxidation of glucose to gluconolactone and hydrogen peroxide[27]. A biosensor consists of three basic components: a biorecognition element (it is a crucial sensing element responsible for selectivity), a transducer (transforms the signal obtained from the molecular interaction between a biological receptor and an analyte to an electrical signal), and electronics for signal transmission in a more user-friendly format (table, graphs, figures, numbers or spectra)[28]. The basic structure of a biosensor is shown in Figure 8. Biosensors are classified depending on the type of transducer such as optical, acoustic, thermal, and electrochemical biosensors. In this thesis an electrochemical biosensor was studied.

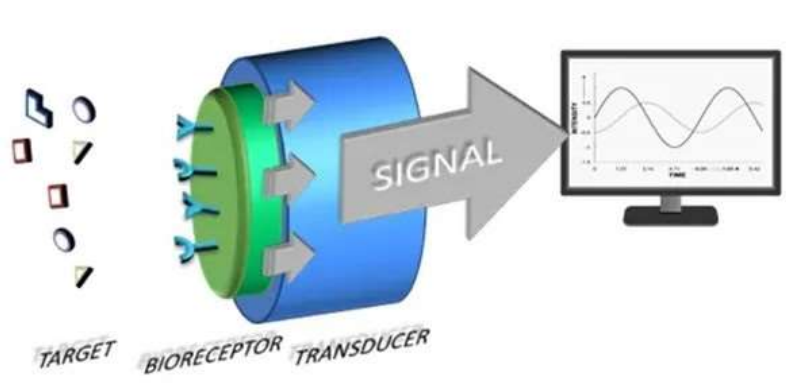


*Figure 8. The basic principle of the biosensor*[29].

### 1.3.1. Electrochemical biosensors

Classical discovery of a glucometer using glucose oxidase-based biosensor is first in the line of discovery of electrochemical biosensors. In 1962 Clark described the detection of glucose by the first amperometric enzymatic electrode. These glucose-sensitive biosensors are commonly used for online control of blood sugar levels in diabetes therapy[30]. Electrochemical sensing has become a promising approach to develop biosensors to detect other biomolecules[31]. Commonly used electrochemical biosensors are based on enzymatic reactions yielding or uptaking charge. Compared to optical, mass and thermal sensors, electrochemical sensors are especially attractive because of their remarkable sensitivity, experimental simplicity and low cost[32]. In an electrochemical sensor a working electrode is modified with a biological receptor capable of forming a stable complex with the target molecule in the analyte solution. Reaction on the WE surface changes electrochemical properties of this electrode, for example by changing surface conductivity. The last effect is easily detectable by current changes in the cell. Two major types of electrochemical sensors are amperometric and potentiometric sensors. In potentiometric sensors, the potential difference between the reference electrode and the working electrode is measured without polarizing the electrochemical cell, that is, very small current is allowed[33]. Amperometric sensors exploit the use of a potential applied between a reference and a working electrode, to cause the oxidation or reduction of an electroactive species; the resultant current is measured[32]. This electric current is a function of the electrochemically active analyte particles that are oxidized or reduced at the surface of the WE and the sensor signal is linearly dependent on the concentration of the analyte. Electrochemical methods are particularly suitable for the direct quantification of redox analytes in solution, as well as for the determination of redox enzymes or their imitations by measuring the formation of electroactive products. The electrochemical sensing methods can be successfully applied also to non-electroactive targets using indirect detection strategies[34]. In these methods changes in the electrochemical signal of an external electroactive compound or redox probe upon the target interaction with a molecular recognition layer present on the electrode surface, are recorded. The more detailed description is provided in Section 1.3.3.

### 1.3.2. Molecularly imprinted polymers based biosensors

As a prospective alternative for unstable biological receptors, synthetic receptors based on molecular imprinted polymers (MIPs) have been extensively studied during the last decades[35,36]. Molecular imprinting technology allows the formation of specific recognition sites or imprints in a synthetic polymer with the memory of an analyte molecule. The general principle of MIP formation is shown in Figure 9. The process includes the polymerization of suitable functional monomers in the presence of a target analyte acting as a template and the subsequent removal of the template by washing with a suitable solvent leading to the formation of binding "pockets", which are complementary to the target molecules in shape, size and location of the functional groups. These "pockets" are capable of reversibly rebinding with target molecules, endowing MIP the capability of selective recognition[4,37].

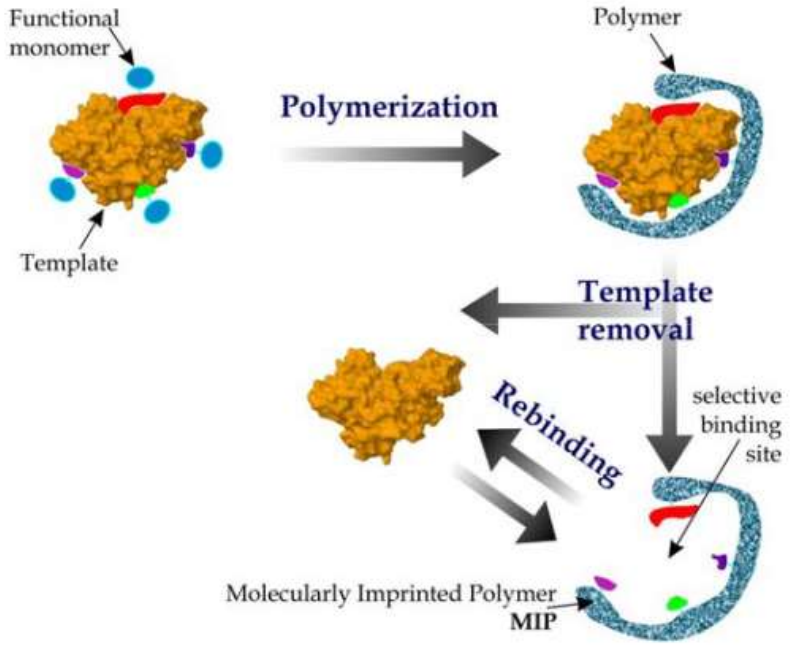


*Figure 9. Scheme of molecularly imprinted polymer (MIP) formation*[38].

MIPs have been considered as inexpensive and robust alternatives for biorecognition elements of biosensors[5]. MIP-based sensors have been widely investigated as promising analytical devices in the field of medical diagnostics aiming the detection of very diverse analytes as biomarkers for early detection of diseases ranging from small molecules[6], to proteins and other biomacromolecules[7], Particularly, MIP-based electrochemical sensors can be considered advantageous due to the simplicity and low cost of the electrochemical transducer, e.g. screen-printed-electrode, as well as the possibility of fast measurement and compatibility with point-of-care testing[8].

Thus, the research group of the laboratory of Biofunctional Materials at TalTech has recently developed MIP-based electrochemical sensors for detection of SARS-CoV-2 viral protein, e.g. nucleocapsid and spike proteins[9,10]. A key element of the sensor is a disposable electrochemical transducer, e.g. thin film electrode, interfaced with a MIP-endowed selectivity to a viral protein and connected with a portable potentiostat. The MIPs were prepared based on the electrochemical surface imprinting approach developed earlier by the research group and successfully used to imprint various proteins[39,40]. Poly(m-phenylenediamine)(PmPD) synthesized by the electrochemical polymerization was used as a polymer matrix for MIP. Electrosynthesis was shown to be a convenient approach for the facile and effective interfacing of protein-MIPs with sensor transducers because the polymeric films can be easily grown with a strict adherence to the electrode surface and the MIP thickness can be easily controlled by the amount of circulated charge[41].

### 1.3.3. Electrochemical readout of MIP-based biosensor

In general, in the case of a MIP-based electrochemical sensor for protein detection, depending on the intrinsic characteristics of the analyte, the transduction can be direct when the redox processes of the target itself and/or its redox-active products are monitored, or indirect when the target is not electroactive and the change in the signal of an external redox probe is monitored[42].

Direct oxidation-reduction of an analyte on the MIP-modified sensor for selective protein detection has been described in few studies[43,44]. However, the indirect method was more commonly used when the target proteins are non-electroactive peptides and proteins. In this method, the electrochemical readout is based on the so-called "gate effect" that arises from affecting the faradaic process of an external redox probe by filling the imprinted cavities of a MIP with analyte molecules[11]. Since the presence of a bulky protein molecule in its molecular cavity can hinder diffusion of small redox probes, the charge transfer at the electrode/solution interface is impeded resulting in the redox current reduction[45]. The reversible redox pair $[Fe(CN)_6]^{3-/4-}$ was commonly used as a redox marker to monitor the indirect response of the MIP- based electrochemical sensor.

The similar detection principle was utilized in the MIP-based biosensor developed in the laboratory of Biofunctional Materials at TalTech for detection of SARS-CoV-2 nucleocapsid protein (ncovNP) (Fig. 10). Namely, the sensing concept relied on the measurement of the changes in DPV current peak related to the inhibition of the charge transfer between the thin-film-electrode (a transducer) and $[Fe(CN)_6]^{3-}/[Fe(CN)_6]^{4-}$ redox probe, through the imprinted pathways created within ncovNP-MIP film. The intensity of the current resulting from the redox reaction of $[Fe(CN)_6]^{3-}/[Fe(CN)_6]^{4-}$ at the MIP-sensor surface was monitored. When the imprinted cavities of ncovNP-MIP were not occupied by the bound protein molecules, the redox probe ions could freely move at the electrode/solution interface and current peak intensity was the highest (blue line in Fig.10). If the film had rebound its target protein (ncovNP) after incubation of the sensor in a sample solution, the charge transfer was efficiently hindered causing a current decrease (red line in Fig.10) that correlated with the concentration of the virus protein in the solution.

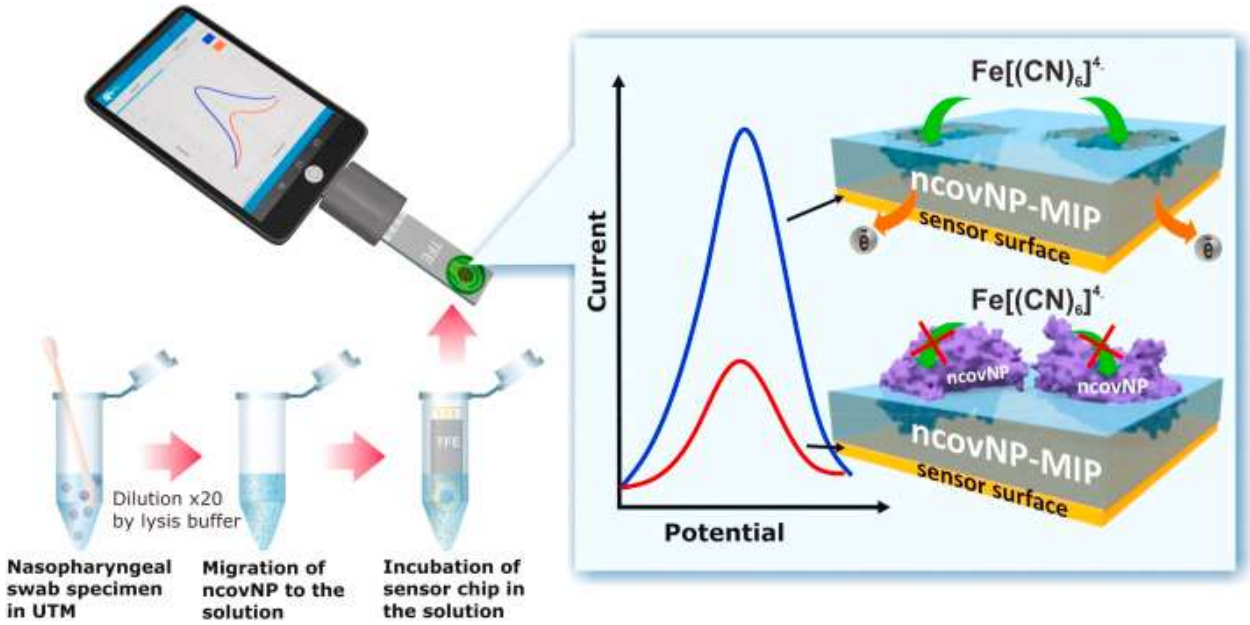


*Figure 10. The detection principle by ncovNP-MIP sensor analyzing the nasopharyngeal swab specimens*[9].

The redox probe solution containing 4mM $[Fe(CN)_6]^{3-/4-}$ and 1 M KCl was used for obtaining the sensor response. As it can be seen the concentration of KCl in the solution is high enough that in the case of its contact with a protein solution, a possible risk to the protein conformation can be expected. It is known that the stability of proteins is affected by salts. Monovalent salts often affect protein stability by modifying the ionic strength of the solution, which can be overall slightly stabilizing or destabilizing, depending on the nature of the specific charge distribution within the protein[46]. Thus, it was reported

that at higher concentrations of neutral salts, the specific lyotropic effect was observed that consisted in the stabilization/destabilization of the native protein conformation, mainly by changing the structure of water and the energy at the solvent-protein[47,48]. Therefore, when developing a MIP-based electrochemical biosensor it is essential to consider the effect of ionic strength of the redox probe solution on the sensor response that can be affected due to the possible conformational change of the target protein. Thus, in order to preserve the nativeness of the protein structure and to improve the sensor response, it is necessary to take into account the electrolyte concentration along with the concentration of the redox pair.

## 1.4. Aims of the thesis

The aim of the thesis is to study the effect of the redox probe solution composition on the MIP-based electrochemical biosensor response. The typical redox probe solution containing 4mM $[Fe(CN)_6]^{3-/4-}$ and 1 M KCl was used so far for electrochemical measurements of the sensor response. Nevertheless, the high concentration of electrolyte can adversely affect the structure or native conformation of protein used as a target analyte and consequently the sensor response[12]. On the other hand, the high supporting electrolyte concentration is necessary to increase the solution conductivity and achieve the charge balance at the electrode/solution interface as well as to prevent charged electroactive species from migrating in the electric field gradient. Thus, simple reduction of the KCl concentration seems to be not a good choice since it can seriously affect the electrochemical signal of the sensor. Therefore, the primary task was to find the optimal redox probe solution composition by varying the concentration of both KCl and a ferri/ferrocyanide probe as well as to study the effect of the solution composition on the MIP-based electrochemical biosensor response. An optimized redox probe solution containing a reduced amount of KCl is expected to provide a similar or even improved sensor response to the target analyte as compared to a previously used redox probe solution. To achieve this aim, the electrochemical behavior of the redox probe solution of different composition at the gold disc electrode was firstly studied. Then, the selected redox probe solution was used to study the adsorption of BSA as a model protein on the bare gold electrode. Finally, the optimized redox probe was used to study the protein rebinding to the MIP-modified gold electrode or, in the other words, MIP-based biosensor. CV and DPV electroanalytical techniques were used to perform the electrochemical measurements in this thesis.

# 2. Experimental part

## 2.1. Chemicals and materials

Potassium ferricyanide ($K_3[Fe(CN)_6]$), potassium ferrocyanide ($K_4[Fe(CN)_6]$), potassium chloride (KCl), sodium chloride (NaCl), disodium hydrogen phosphate, 4-aminothiophenol (4-ATP), 2-mercaptoethanol(2-ME), m-phenylenediamine(m-PD), acetic acid(AA), and bovine serum albumin (BSA) were purchased from Sigma-Aldrich. 3,3′-dithiobis[sulfosuccinimidylpropionate] (DTSSP) was purchased from Thermo Fisher Scientific Inc. Sulfuric acid, hydrogen peroxide, and potassium chloride were purchased from Lach-ner, S.R.O. All chemicals were of analytical grade or higher and were used as received without any further purification. Phosphate buffered saline (PBS) pH 7.4 ($Na_2HPO_4$ 10 mM, $KH_2PO_4$ 1.8 mM, NaCl 137 mM, KCl 2.7 mM) and ultrapure Milli-Q (MQ) water (resistivity 18.2 MΩ cm at 25 °C, Merck KGaA, Darmstadt, Germany) were used for the preparation of all aqueous solutions.

## 2.2. Solutions preparation

The salt solutions (KCl, $K_3[Fe(CN)_6]$ and $K_4[Fe(CN)_6]$) in MQ and PBS were used to prepare the probes solutions for electrochemical measurements. Aiming at probe solution optimization, we searched for solutions with variable salt concentrations in MQ water and PBS. KCl concentrations were varied in the range of 0.1 to 1M at a fixed concentration of $[Fe(CN)_6]^{3-/4-}$ (4 or 12 mM) and the concentrations of $[Fe(CN)_6]^{3-/4-}$ were varied in the range of 4 to 20mM in PBS or in MQ at a fixed concentration of KCl (0.3 M). BSA solutions were prepared by diluting the protein in PBS at an initial concentration of 1 mg/mL followed by 10 fold serial dilution to a concentration of $10^{-9}$ mg/mL.

The conductivity of the solutions were measured with the conductometer Seven Compact from Mettler Toledo. The ionic strength of the prepared solutions calculated from the equation:

$$I = \frac{1}{2}\sum_{i=1}^{n} C_i z_i^2,$$

where
$I$ - ionic strength
$C_i$ - concentration of ion
$z_i$ - ion charge

## 2.3. Electrode modification with MIP

The procedure of protein-MIP synthesis on the gold surface of the WE was adapted from the previous work of the research group[10]. BSA was selected as a model protein in this study. In order to immobilize covalently BSA on the gold surface of WE, the cleaned electrode was immersed in an ethanolic solution of 0.1M 4-ATP followed by incubation in a 10mM DTSSP solution and finally in 1 mg/mL BSA solution in PBS. The duration of each step was 30 minutes. The electrodeposition of poly(m-phenylenediamine) (PmPD) on BSA-modified WE was performed from PBS containing 10mM mPD at vs Ag/AgCl/KCl until the charge density of 2 mC/cm$^2$ was achieved. Molecular imprints of BSA in the polymer film were generated by treating the polymer film with an ethanolic solution of 0.1M 2-ME with heating at 80$^0$C for

1 hour to cleave the S–S bond of DTSSP and facilitate the release of BSA, followed by washing with a 10% acetic acid solution for 30 minutes to dissociate non-covalent bonds between the polymer and the protein. Figure 11 outlines the scheme of the BSA-MIP synthesis of the gold electrode.

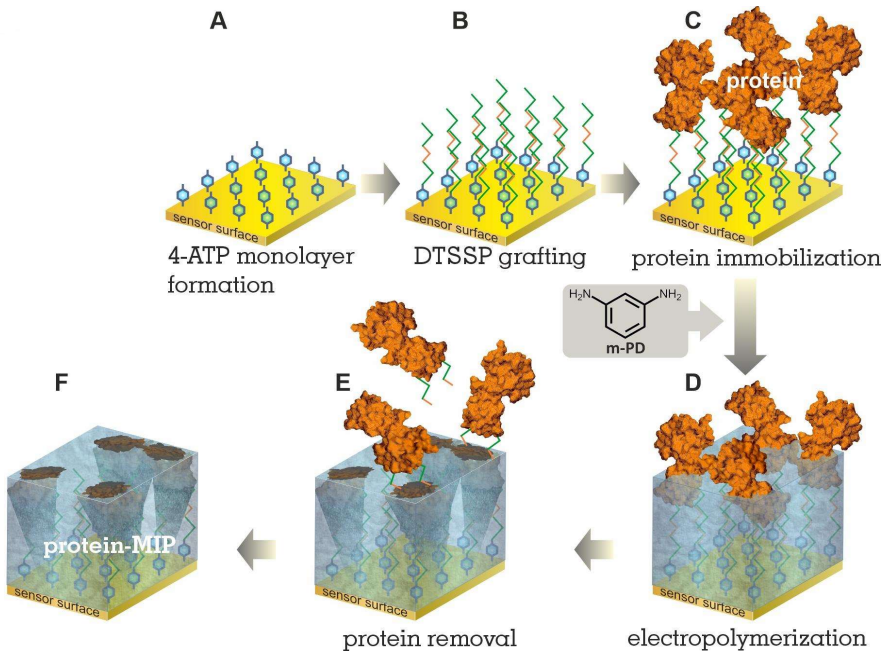


*Figure 11. General scheme of gold surface modification with MIP and all processes. (A) assembling a 4-ATP monolayer with an Au electrode; (B) attachment of DTSSP cleavable linker; (C) protein covalent immobilization; (D) electropolymerization; (E) washing out the protein molecules with Me/EtOH and AA; (F) rebinding of protein (adapted from [40]).*

## 2.4. Electrochemical measurements

Electrochemical measurements were made in a 40 mL glass electrochemical cell (Figure 12) connected with Reference 600 Potentiostat (Gamry Instruments, USA). A conventional three-electrode system was used with a gold disc electrode with a diameter of 2mm as WE, a platinum wire as CE, and a $Ag/AgCl/KCl_{sat}$ as RE. Before the measurement the gold surface of WE was cleaned by immersion in fresh piranha solution (97%$H_2SO_4$ : 30%$H_2O_2$, 3:1 volume ratio) for 7 minutes and then rinsed abundantly with MQ water and dried. This step was performed under the fume hood. Electrochemical behavior of $[Fe(CN)_6]^{3-/4-}$ redox probe in electrolyte solution of different concentrations on the bare gold electrode was studied by CV. The cyclic voltammograms were registered by cycling the potential between 0.1 and 0.5 V at a scan rate of 50 mV/s or at varying scan rate in the range of 50-500 mV/s. Gold electrode modification steps during MIP preparation were characterized electrochemically by CV in a redox probe solution, which can be found in Appendix 3. To study the BSA adsorption on bare gold or on MIP, the cleaned WE or MIP-modified WE, respectively, was immersed for 15 minutes in PBS solution containing BSA at varying concentrations ($10^{-9}$ mg/mL - 1 mg/mL). Then the electrode was rinsed with PBS, dipped into the $[Fe(CN)_6]^{3-/4-}$ redox probe solution and DPV measurements were carried out. The measurement parameters include a potential range of 0 - 0.5 V, pulse amplitude of 25 mV, pulse width of 0.1 s, a step potential 5 mV and sample period of 0.1 s. The measurements settings of CV and DPV can be found in Appendices 1 and 2.

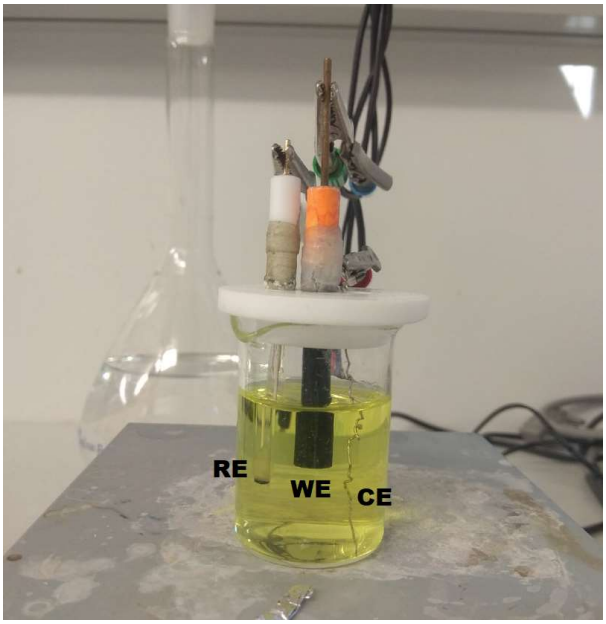


*Figure 12. Experimental electrochemical cell.*

# 3. Results and discussion

## 3.1. Effect of electrolyte concentration on redox probe electrochemical behavior

The electrochemical measurements are usually performed in a supporting electrolyte solution that is electrochemically inert and fulfills two very important purposes. First, the supporting electrolyte decreases the electrical resistance of the cell that reduces the Ohmic drop effect. The second role of the supporting electrolyte is to suppress the migration of electro-active species towards the electrodes through electrostatic attractions to achieve diffusion-controlled currents[49]. Usually, the concentration of the supporting electrolyte should be high enough to accomplish the task. Thus, the solution of KCl at a concentration of 1M has been widely used to prepare the redox probe solution for voltammetric measurements. Such solution was also used for electrochemical readout of the laboratory developed MIP-based sensor for detection of selected proteins. However, high concentration of a neutral salt can affect the native conformation of proteins, alternating the protein rebinding process to the MIP and consequently the electrochemical sensor response[12].

The optimization of the redox probe solution has been started with the attempt to reduce the concentration of KCl while keeping constant the concentration of $[Fe(CN)_6]^{3-/4-}$. The cyclic voltammograms of a bare gold electrode registered in electrolyte solution containing 4 mM $[Fe(CN)_6]^{3-/4-}$ and various concentrations of KCl in the range of 0 to 1 M are presented in Figure 13(a) and the derived parameters are summarized in Table 1. As it can be seen the voltammogram in the absence of electrolyte has not well-defined faradaic peaks with a large redox peak potential difference (ΔE). This indicates the slow charge transfer kinetics at the electrode/solution interface due to the solution resistance in the absence of the electrolyte. When the KCl is added to the solution, the well-defined oxidation and reduction peaks corresponding to the oxidation $[Fe(CN)_6]^{4-}$ ions and the reduction of the $[Fe(CN)_6]^{3-}$ ions, respectively, appear on the voltammograms. Moreover, the ΔE value progressively decreases (from 144 to 88 mV) with increasing the concentration of the supporting electrolyte from 0.1 to 1.0 M indicating the improvement in the efficiency of the electron transfer process due to the reducing the electrolyte resistance. However, it should be noted that the lowest ΔE value of 88 mV obtained for 1.0 M KCl is greater compared to the expected theoretical value (59 mV at 25 °C) for a reversible and diffusion-controlled one electron-transfer process. This indicates that the uncompensated resistance effect (e.g. the Ohmic drop effect) cannot be considered negligible even at high concentrations of electrolyte solutions[49]. In addition, this can be affected by electrode preparation and potential scan rate. It can be also observed that the current peak intensity for both anodic and cathodic reactions increased more rapidly with increasing KCl concentration from 0.1 to 0.3M but after that remains practically unchanged in 0.3-1.0 M KCl solution. At the same time, the significant difference in current peak intensities at these concentrations can be observed on DPV plots in Figure 13(b). The lower the KCl concentration the lower the DPV peak intensity. Since, the DPV peak intensity is the main parameter of the electrochemical biosensor, we decided to increase the concentration of the redox pair in order to obtain the similar peak intensity at lower KCl concentration in the optimized redox probe solution.

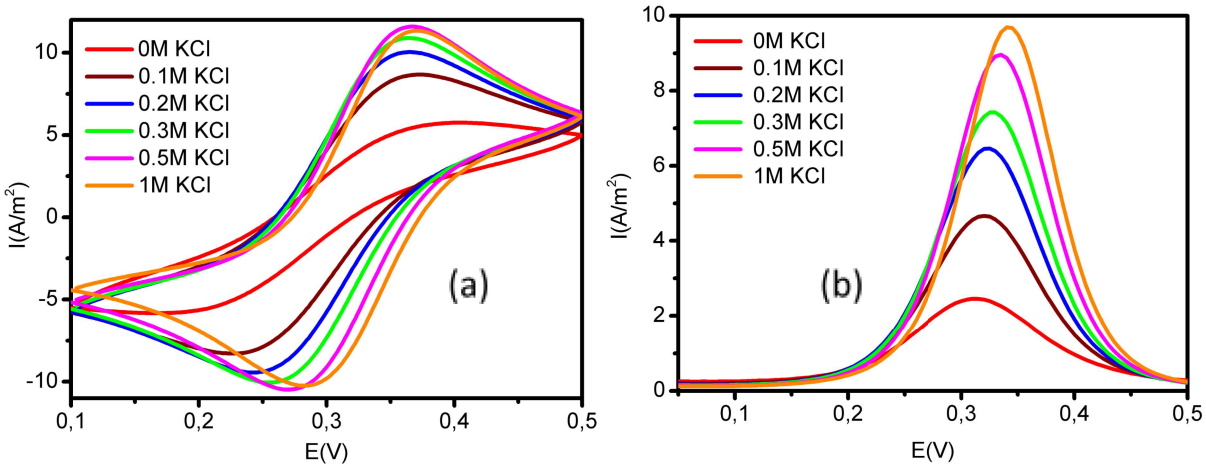


*Figure 13. Cyclic voltammograms (a) and DPV plots (b) of a bare gold disk electrode in aqueous solution containing 4mM $[Fe(CN)_6]^{3-/4}$ and different concentrations of KCl between 0 and 1M. Cyclic voltammograms were recorded at a scan rate of 50 mV/s.*

We selected the electrolyte concentration as 0.3 M KCl and we started to increase the concentration of $[Fe(CN)_6]^{3-/4-}$ from 4 mM to 20 mM. In Figure 14 we can see that as expected, the intensity of anodic and cathodic peak current on the cyclic voltammograms and the intensity of DPV peak current increase with increasing the redox pair concentration. Also, it can be seen that the DPV peak intensity at 12mM $[Fe(CN)_6]^{3-/4}$ in 0.3M KCl is a little bit higher than in the solution of 4mM $[Fe(CN)_6]^{3-/4}$ in 1.0M KCl. Although the highest DPV intensity was obtained in 20mM $[Fe(CN)_6]^{3-/4}$ solution, it was considered too high for the electrochemical biosensor in this study due to the possible negative impact on protein conformation[50]. We also tried to perform the similar measurements in the PBS solution without addition of KCl. As it can be seen in Figure 15 the cyclic voltammograms have not well-defined faradaic peaks with a large redox peak potential difference (ΔE), indicating the slow charge transfer kinetics at the electrode/solution interface. Although the PBS already contains salts such as KCl and NaCl, their concentration is not enough for reducing the solution resistance and ensuring the fast charge transfer at the interface.

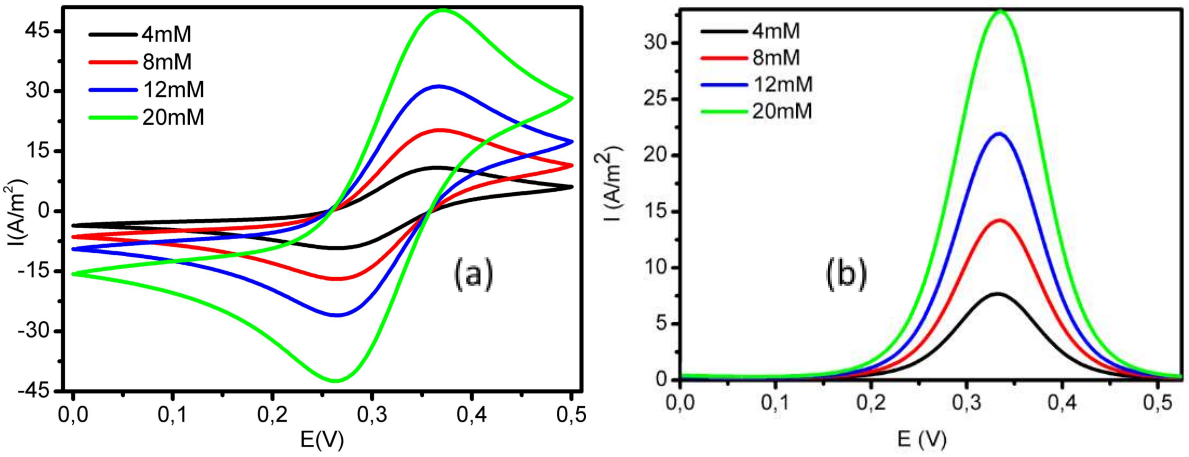


*Figure 14. Cyclic voltammograms (a) and DPV plots (b) of bare gold disk electrode in aqueous solution containing 0.3M KCl and different concentrations of $[Fe(CN)_6]^{3-/4-}$ between 4 and 20 mM Cyclic voltammograms were recorded at a scan rate of 50 mV/s.*

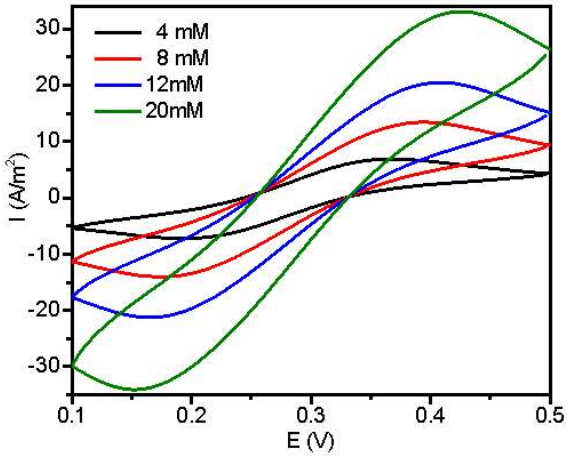


*Figure 15. Cyclic voltammograms of a bare gold disk electrode in PBS solution containing different concentrations of $[Fe(CN)_6]^{3-/4-}$ between 4 and 20mM. Scan rate 50 mV/s.*

In addition, the CV and DPV measurements in 12mM $[Fe(CN)_6]^{3-/4-}$ solution with different concentrations of KCl were performed (Fig.16). We can see on the voltammograms (Fig.16(a)) the similar behavior as in the case of the 4mM redox pair in solutions with different concentrations of KCl (Fig.14(a)). Namely, the absence of the redox peaks in the solution without KCl, the appearance of the reversible redox peak pair when electrolyte was added and the decrease of the ΔE value with increasing electrolyte concentration were observed (Fig.16(a) and Table 1). The DPV shows the well-defined peaks with current intensity increase with increasing electrolyte concentration (Fig.16(b)).

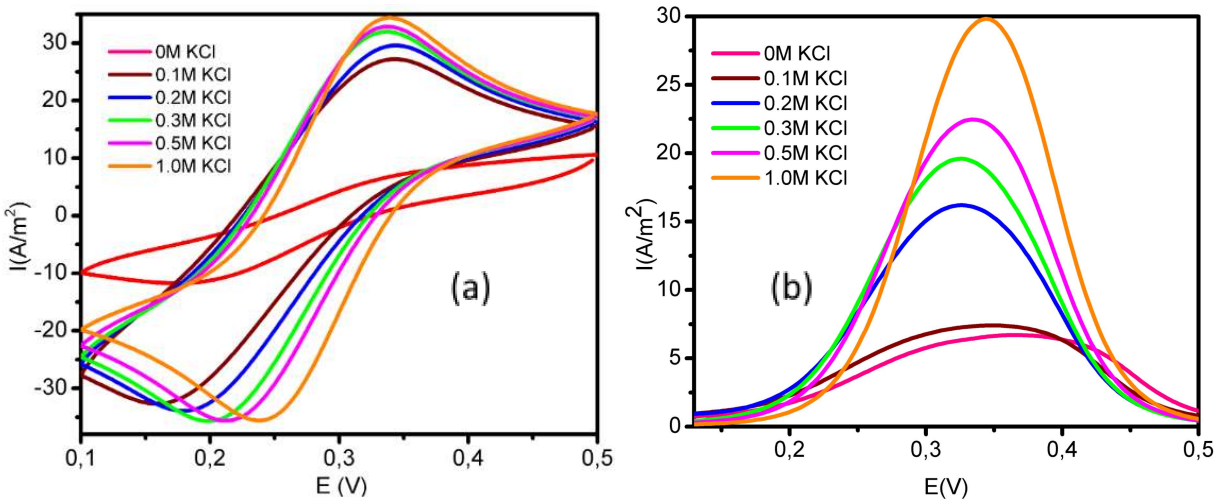


*Figure 16. Cyclic voltammograms (a) and DPV plots (b) of bare gold disk electrode in aqueous solution containing 12 mM $[Fe(CN)_6]^{3-/4-}$ and different concentrations of KCl between 0 and 1M Cyclic voltammograms were recorded at a scan rate of 50 mV/s.*

**Table 1.** The parameters derived from the cyclic voltammograms presented in Figures 13(a) and 16(a).

| Conc of KCl, M* | $E_a$, mV | $E_c$, mV | $\Delta E_p$, mV | $E_{1/2}$, mV | $I_a$, A/m$^2$ | $I_C$, A/m$^2$ |
|---|---|---|---|---|---|---|
| $[Fe(CN)_6]^{3-/4-}$ at 4mM | | | | | | |
| 0 | 402 | 164 | 238 | 283 | 5.8 | 5.8 |
| 0.1 | 372 | 228 | 144 | 300 | 8.7 | 8.2 |
| 0.2 | 364 | 242 | 122 | 303 | 10.0 | 9.4 |
| 0.3 | 364 | 256 | 108 | 310 | 10.9 | 10.1 |
| 0.5 | 366 | 270 | 96 | 318 | 11.6 | 10.5 |
| 1.0 | 370 | 282 | 88 | 326 | 11.3 | 10.2 |
| $[Fe(CN)_6]^{3-/4-}$ at 12mM | | | | | | |
| 0 | 500 | 176 | 324 | 338 | 7.1 | 8.0 |
| 0.1 | 342 | 158 | 184 | 250 | 18.6 | 22.3 |
| 0.2 | 344 | 180 | 164 | 262 | 20.2 | 23.1 |
| 0.3 | 336 | 198 | 138 | 267 | 21.8 | 24.4 |
| 0.5 | 338 | 212 | 126 | 275 | 22.4 | 24.3 |
| 1 | 338 | 238 | 100 | 288 | 23.5 | 24.4 |

Based on the above mentioned results we decided to select the solution of 12mM $[Fe(CN)_6]^{3-/4-}$ in 0.3M KCl for the subsequent study. In order to simplify the designation of the redox probe solutions we introduced the following abbreviations:
TPS - traditional probe solution containing, 4 mM $[Fe(CN)_6]^{3-/4-}$ and 1 M KCl;
UPS - upgraded probe solution containing 12 mM $[Fe(CN)_6]^{3-/4-}$ and 0.3 M KCl.

The next step was the determination of the diffusion coefficient of $[Fe(CN)_6]^{3-/4-}$ species in TPS and UPS. The diffusion coefficient is a parameter, which determines the mobility of a diffusing substance in a solution. For the diffusion-controlled reversible charge transfer process, the Randles-Sevcik equation describes the effect of scan rate and diffusion coefficient on the peak current[21]:

$$i_p = 0,4463nFAc\sqrt{vD\frac{nF}{RT}},$$

where $i_p$ is the peak intensity (mA), $v$ the scan rate (V/s), $n$ the number of electrons transferred in the surface reaction, $A$ the electrode area (cm$^2$), $D$ the diffusion coefficient of ferricyanide ions (cm$^2$/s), and $c$ its concentration in the bulk solution (mol/cm$^3$). At room temperature (25 °C), it becomes[21]:

$$i_p = (2,6865 * 10^5)Ac\sqrt{vD}$$

Using the relationships defined by this equation, the diffusion coefficient of electroactive species ($[Fe(CN)_6]^{3-}$and $[Fe(CN)_6]^{4-}$) can be determined with a plot of $i_p$ vs. $\sqrt{v}$, which should be linear when the system is reversible. Therefore, the CV curves in both TPS and UPS solutions over a wide range of the scan rates, 50-500 mV/s were recorded (Fig.16) and the peak current ($i_p$ ) versus the square root of scan rate ($\sqrt{v}$) was plotted (Fig. 17(c)).

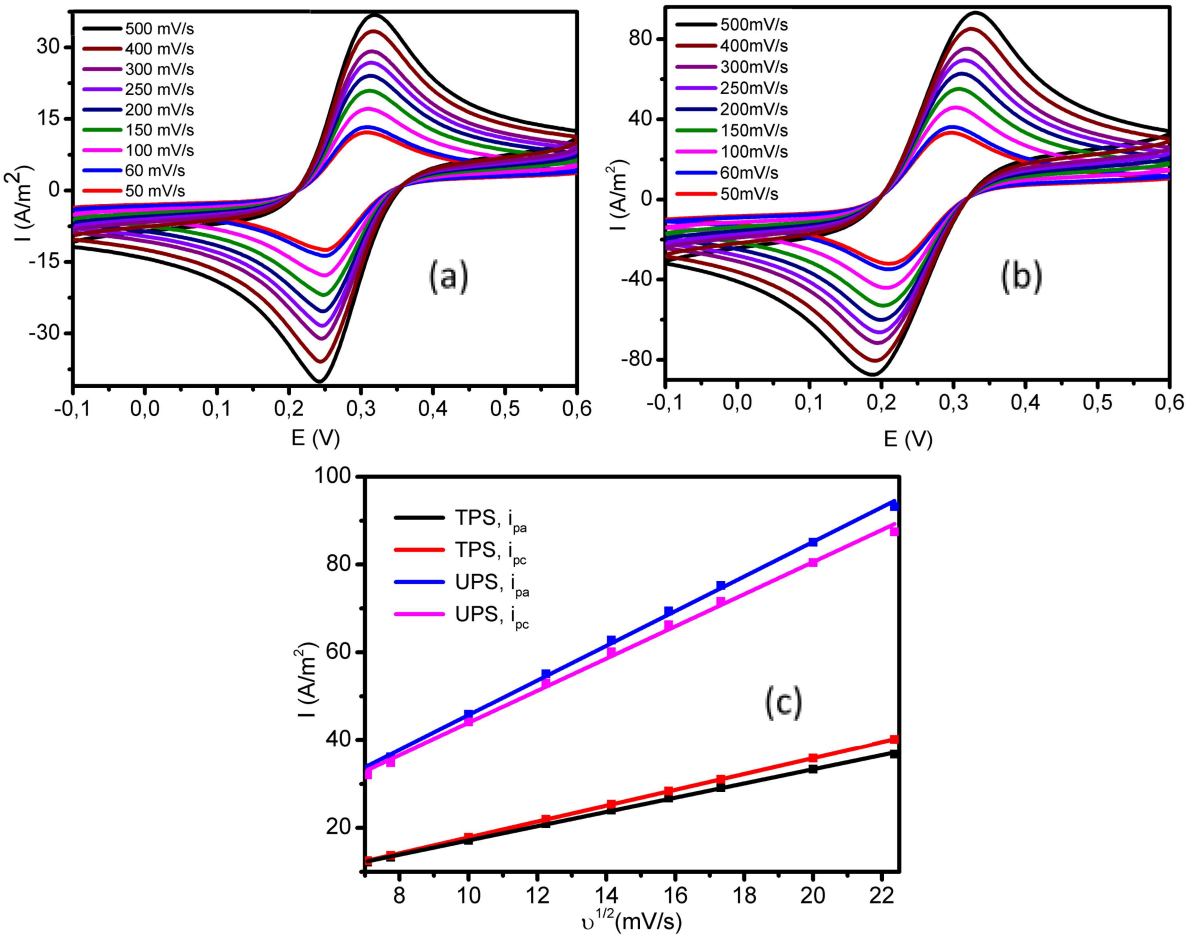


*Figure 17. Cyclic voltammograms of a bare gold disk electrode recorded at different scan rates from 50 to 500 mV/s in (a) TPS solution and (b) UPS solution and (c) plots of the peak current versus the square root of scan rate.*

The results showed that the anodic and cathodic peak currents are in linear relationship with the square root of the scan rates indicating that the electrode reactions of $[Fe(CN)_6]^{3-/4-}$ redox probe is a diffusion-controlled process in both TPS and UPS solutions. The diffusion coefficients calculated from the slope of linear plots in Fig.17(c) were as follows: $5.70*10^{-6}$ $cm^2/s$ for $[Fe(CN)_6]^{3-}$and $7.07*10^{-6}$ $cm^2/s$ for $[Fe(CN)_6]^{4-}$ in TPS and $1.80*10^{-6}$ $cm^2/s$ for $[Fe(CN)_6]^{3-}$and $3.23*10^{-6}$ $cm^2/s$ for $[Fe(CN)_6]^{4-}$ in UPS. The obtained values agree well with the literature reports[51].

The determined diffusion coefficient values as well as the conductivities and ionic strength values for TPS and UPS solutions are summarized in Table 2. The results demonstrated that by lowering three times the concentration of KCl and increasing by three times the concentration of the redox pair we obtained the redox probe solution with two times lower ionic strength as compared to TPS. The

conductivity of UPS, as expected, was two times lower than that of TPS and the values of the *D* for $[Fe(CN)_6]^{3-/4-}$ in UPS were slightly smaller while of the same order of magnitude as compared to that in TPS. Nevertheless, the CV and DPV measurements demonstrated that the reversibility and the charge transfer kinetics of the redox probe reaction were comparable for TPS and UPS solutions. Therefore, we selected UPS as an optimal redox probe solution for the subsequent measurement of MIP-based biosensor response.

**Table 2.** The values of conductivity, ionic strength and diffusion coefficients for UPS and TPS.

| **Parameter** | **UPS** | **TPS** |
|---|---|---|
| The conductivity, µS/cm | 58.7 | 120.0 |
| Ionic strength, mM | 492 | 1064 |
| The diffusion coefficient, $10^{-6}$ $cm^2/s$, of:<br>$[Fe(CN)_6]^{3-}$<br>$[Fe(CN)_6]^{4-}$ | <br>1.80<br>3.23 | <br>5.70<br>7.07 |

## 3.2. Electrochemical study of protein adsorption on gold electrode

Firstly, the selected redox probe solution - UPS - was applied to study the adsorption of a model protein - BSA - on a bare gold electrode. DPV measurements were carried out in UPS and TPS (for comparison) after the incubation of the gold electrode in PBS containing BSA at concentration in the range from $10^{-9}$ mg/mL to 1 mg/mL (Fig. 18). As it can be seen in Figure 18 the DPV peak current intensity is maximal after incubation in a blank PBS solution (without BSA) and decreases with increasing protein concentration in PBS. This is attributed to the gradual blocking of the electrode surface by the adsorbed protein molecules after the incubation in PBS with increasing protein concentration.

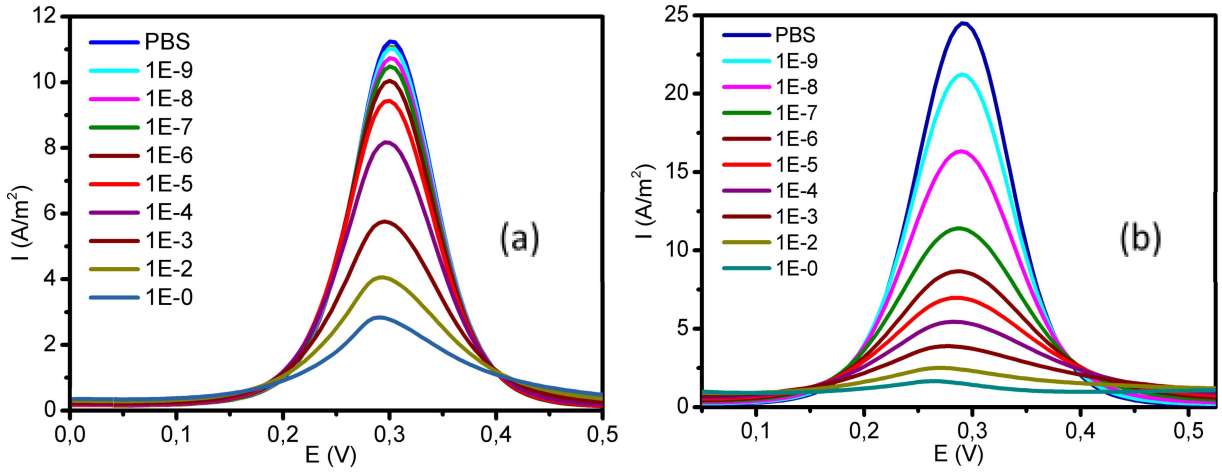


*Figure 18. DPV recorded plots in (a) TPS and; (b) UPS after incubation of a gold electrode in PBS with different BSA concentrations.*

The recorded DPV current peaks were normalized to obtain the normalized response signals ($I_n$), which can be used for analyzing the blockage by the protein on the WE, according to the following equation:

$$I_n = \frac{I_0 - I}{I_0},$$

where

$I_0$ - initial peak current intensity after incubation in blank PBS solution

$I$ - peak current intensity after incubation in PBS containing a particular concentration of protein

The normalized current response has an inverse relationship with the actual measurement i.e the normalized response increases with increasing concentration of analyte. The dependence of the normalized DPV responses on the BSA concentration is presented in Figure 19 for TPS and UPS solutions. It is possible to observe that the signals in UPS are greater than that recorded in TPS for all concentrations of BSA. The difference is more significant at the lower protein concentration up to $10^{-4}$ mg/mL. This indicates that the use of UPS can allow detection of BSA at a lower concentration as compared to the measurement in TPS. Based on the obtained results, we can see that the effectiveness of the UPS shows better results at determining concentrations as low as $10^{-9}$ mg/mL. We also see a saturation of the protein on the electrode with increasing concentration is achieved earlier (at lower concentration) in UPS as compared to TPS.

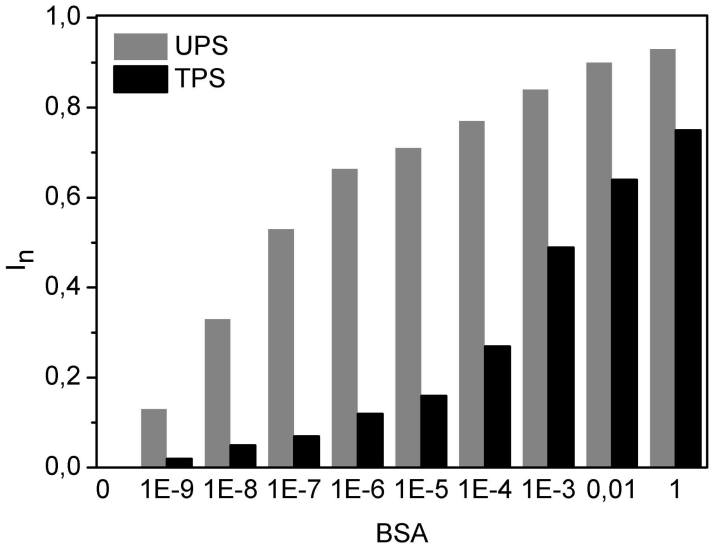


*Figure 19. The normalized DPV responses obtained after incubation of a bare gold electrode in BSA solution of different concentrations: from $10^{-9}$ mg/mL to 1 mg/mL.*

## 3.3. Electrochemical study of protein rebinding on MIP-modified gold electrode

To prepare the biosensor, the gold electrode was modified with a MIP-based synthetic receptor endowing selectivity towards the target protein - BSA in this study. The BSA-MIP was synthesized using the electrochemical surface imprinting approach developed in the laboratory[40] and described in Section 2.3 of the manuscript. All electrode modification steps during MIP formation were monitored by CV measurements using TPS and UPS as redox probe solutions (see Appendix 3). It can be seen that the modification of the gold electrode with 4-ATP monolayer almost did not affect current peaks of the redox couple in TPS and UPS. However, after the subsequent attachment of DTSSP, and BSA the redox current peaks were gradually reduced due to the hindering of the charge transfer process because of

the insulating nature of the deposited organic layers. Moreover, after electrodeposition of poly(m-PD), the peaks completely disappeared, indicating the formation of a non-conducting polymer film on the electrode. After the subsequent template removal (washing out) process, which includes the steps of destroying disulfide bond of DTSSP with 2-ME and treatment in AA solution, a re-emergence of the CV anodic and cathodic peaks was observed indicating supposedly, elution of BSA from the polymer and formation of molecular imprints, which tunneled the charge transfer across the ultra-thin non-conducting PmPD layer to the electrode[9,10]. Thus, it was demonstrated that the selected redox probe solution, UPS, is suitable for the electrochemical characterization of the MIP formation on the electrode surface.

To measure the response of the prepared MIP-based sensor towards the target protein (BSA), the BSA-MIP-modified electrode was incubated in PBS containing BSA at concentration in the range from $10^{-9}$ mg/mL to 1 mg/mL and then DPV measurements were carried out in UPS and TPS (for comparison) (Fig. 20).

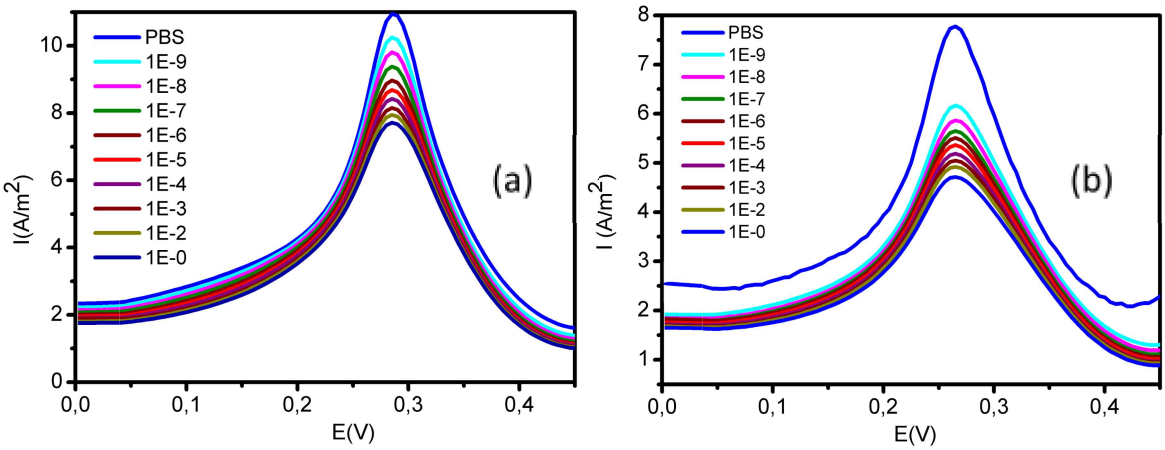


*Figure 20. DPV plots recorded in (a) TPS and (b) UPS after incubation of MIP-modified gold electrode in PBS with different BSA concentrations.*

Similarly to BSA adsorption on bare gold, the gradual decrease of DPV peak current with increasing concentration of BSA was observed in the case of the MIP-modified electrode. While in this case the value of peak current density was much lower, obviously due to the insulating character of the MIP layer. At the same time it can be seen that the DPV current intensities recorded in TPS and UPS solutions were similar despite the fact that UPS contained 3 times more of $[Fe(CN)_6]^{3-/4-}$. The plots of the normalized DPV responses as a function of BSA concentration (Fig. 21) demonstrated a more significant difference in the signal obtained in UPS and TPS at the lower protein concentration. Thus, the sensor responses measured in UPS were more than 1.5 times higher as compared to that measured in TPS for the BSA concentrations in the range $10^{-9}$ - $10^{-7}$ mg/mL. This indicates that the use of UPS allows detection of BSA by MIP-sensor at a lower concentration as compared to the measurement in TPS, thus enhancing the measurement sensitivity. We can also notice that despite the different efficiency of the UPS and TPS solutions, the saturation of the BSA-MIP was achieved around the same levels in the range $10^{-4}$ mg/mL - 1 mg/mL.

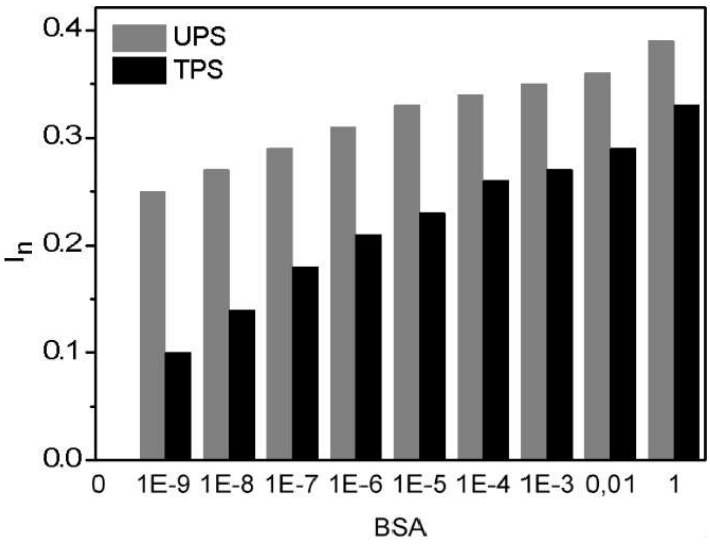


*Figure 21. The normalized DPV responses obtained after incubation of MIP-modified gold electrode in BSA solution of different concentrations: from $10^{-9}$ mg/mL to 1 mg/mL.*

# 4. Conclusions

The aim of the thesis was to study the effect of the redox probe solution composition on the MIP-based electrochemical biosensor response to find the optimal solution composition. An optimized redox probe solution was supposed to contain a reduced amount of KCl as compared to the traditional redox probe solution (TPS) while possessing the similar electrochemical behavior and not significantly affecting the electrochemical response of the sensor. CV and DPV electroanalytical techniques were used as the main methods for performing electrochemical measurements in this study. First, the electrochemical behavior of the redox probe solution of different concentrations of KCl (0.1 - 1.0M) and $[Fe(CN)_6]^{3-/4-}$ (4 - 20 mM) redox pair at the gold disc electrode was studied, aiming to identify an optimal solution composition with a reduced concentration of KCl. Based on the experimental results, the upgraded redox probe solution (UPS), containing 3 times decreased concentration of KCl (0.3M), and 3 times increased concentration of $[Fe(CN)_6]^{3-/4-}$ couple (12mM) as compared to TPS was selected as optimal. A noticeable decrease of salt concentrations was expected to maintain the stability of the studied BSA protein, but the increase in the $[Fe(CN)_6]^{3-/4-}$ redox pair allowed to obtain the similar DPV peak intensity at lower KCl concentration. The values of diffusion coefficient of $[Fe(CN)_6]^{3-/4-}$ species in TPS and UPS were determined from the dependence of current peak intensity from the square root of scan rate. The results showed that the anodic and cathodic peak currents were in linear relationship with the square root of the scan rates indicating that the electrode reactions of $[Fe(CN)_6]^{3-/4-}$ redox probe is a diffusion-controlled process in both solutions. The calculated diffusion coefficients were as follows: $5.70*10^{-6}$ $cm^2/s$ for $[Fe(CN)_6]^{3-}$and $7.07*10^{-6}$ $cm^2/s$ for $[Fe(CN)_6]^{4-}$ in TPS and $1.80*10^{-6}$ $cm^2/s$ for $[Fe(CN)_6]^{3-}$and $3.23*10^{-6}$ $cm^2/s$ for $[Fe(CN)_6]^{4-}$ in UPS. It was found that the ionic strength of the UPS was two times lower than that of TPS: 492 mM for UPS and 1064 mM for TPS. The conductivity of UPS was also two times lower than that of TPS: 58.7 µS/cm for UPS and 120.0 µS/cm for TPS. Nevertheless, the CV and DPV measurements demonstrated that the reversibility and the charge transfer kinetics of the redox probe reaction were comparable for TPS and UPS solutions. Therefore, we selected UPS as an optimal redox probe solution for the subsequent measurement of MIP-based biosensor response.

Preliminary DPV measurements in UPS and TPS were carried out in order to study the adsorption of a model protein (BSA) on a bare gold electrode. The concentration of BSA varied in the range from $10^{-9}$ mg/mL to 1 mg/mL. The results demonstrated that the DPV normalized signals in UPS were greater than that in TPS for all concentrations of BSA. The difference was more significant at the lower protein concentration up to $10^{-4}$ mg/mL. This proved that UPS can detect the adsorption of BSA on bare gold at a lower concentration as compared to the measurements in TPS.

Then, a MIP-based electrochemical biosensor was prepared by modifying the gold electrode with BSA-MIP as a synthetic receptor against BSA. All electrode modification steps during MIP formation were monitored by CV measurements using TPS and UPS as redox probe solutions. It was demonstrated that the UPS is suitable for the electrochemical characterization of the MIP formation on the electrode surface. The BSA-MIP biosensor responses were obtained by DPV measurements in UPS and TPS upon incubation of the sensor in PBS containing BSA in the concentration range from $10^{-9}$ mg/mL to 1 mg/mL. It was found that the sensor responses measured in UPS were more than 1.5 times higher as compared to that measured in TPS for the BSA concentrations in the range $10^{-9}$ - $10^{-7}$ mg/mL. This indicates that the use of UPS allows detection of BSA by MIP-biosensor at a lower concentration as compared to the measurement in TPS, thus increasing the measurement sensitivity.

In summary, the redox probe solution (UPS) with optimized composition of KCl and $[Fe(CN)_6]^{3-/4}$ was shown to be suitable for analyzing the response of MIP-biosensors. Due to the decreased salt concentration, the UPS solution is expected to be less affecting the native conformation of protein during the measurement procedure than the previous probe solution (TPS). Thus, in further studies in the laboratory of Biofunctional materials at TalTech, a new optimized solution can be used for the development of protein-MIP biosensors. The data and results, which have been collected and analyzed in this study, can be used for future research aiming to improve the electrochemical readout of the MIP-based biosensor. For example, along with $[Fe(CN)_6]^{3-/4-}$ containing redox probe solution the other redox pairs, such as rubidium complex salt $[Ru(NH_3)_6]^{2+/3+}$ or ferrocene/ferrocenium can be studied.

## Acknowledgments

First of all, I want to deeply thank my supervisor **Jekaterina Reut**, for her supervision of my thesis, help in writing and analyzing the results, I also want to thank her for her patience and giving such needed advice for me, when I was her student. I was very lucky to have such a good leader and teacher, who was really interested in this topic and work, who was able to explain in great detail to me the important details of this subject.

I also want to thank **Roman Borozнjak** for his great assistance in the practical part of the thesis. I thank him for these tips, help in compiling graphs, tables and important data.

I also want to thank everybody who accepted me into their team at the Laboratory of Biofunctional Materials at TalTech.

Lastly, I want to thank my **family** and **friends** who supported me and always cheered me up.

# References


(1) Rinken, T.; Kivirand, K. *Biosensors for Environmental Monitoring*; 2019. https://doi.org/10.5772/intechopen.73763.

(2) Saylan, Y.; Özgür, E.; Denizli, A. Recent Advances of Medical Biosensors for Clinical Applications. *Med. DEVICES Sens.* **2021**, *4* (1), e10129. https://doi.org/10.1002/mds3.10129.

(3) Vigneshvar, S.; Sudhakumari, C. C.; Senthilkumaran, B.; Prakash, H. Recent Advances in Biosensor Technology for Potential Applications – An Overview. *Front. Bioeng. Biotechnol.* **2016**, *4*.

(4) Alexander, C.; Andersson, H. S.; Andersson, L. I.; Ansell, R. J.; Kirsch, N.; Nicholls, I. A.; O'Mahony, J.; Whitcombe, M. J. Molecular Imprinting Science and Technology: A Survey of the Literature for the Years up to and Including 2003. *J. Mol. Recognit.* **2006**, *19* (2), 106–180. https://doi.org/10.1002/jmr.760.

(5) Ertürk, G.; Mattiasson, B. Molecular Imprinting Techniques Used for the Preparation of Biosensors. *Sensors* **2017**, *17* (2), 288. https://doi.org/10.3390/s17020288.

(6) Elugoke, S. E.; Adekunle, A. S.; Fayemi, O. E.; Akpan, E. D.; Mamba, B. B.; Sherif, E.-S. M.; Ebenso, E. E. Molecularly Imprinted Polymers (MIPs) Based Electrochemical Sensors for the Determination of Catecholamine Neurotransmitters – Review. *Electrochem. Sci. Adv.* **2021**, *1* (2), e2000026. https://doi.org/10.1002/elsa.202000026.

(7) Di Giulio, T.; Mazzotta, E.; Malitesta, C. Molecularly Imprinted Polyscopoletin for the Electrochemical Detection of the Chronic Disease Marker Lysozyme. *Biosensors* **2021**, *11* (1), 3. https://doi.org/10.3390/bios11010003.

(8) Crapnell, R. D.; Dempsey-Hibbert, N. C.; Peeters, M.; Tridente, A.; Banks, C. E. Molecularly Imprinted Polymer Based Electrochemical Biosensors: Overcoming the Challenges of Detecting Vital Biomarkers and Speeding up Diagnosis. *Talanta Open* **2020**, *2*, 100018. https://doi.org/10.1016/j.talo.2020.100018.

(9) Raziq, A.; Kidakova, A.; Boroznjak, R.; Reut, J.; Öpik, A.; Syritski, V. Development of a Portable MIP-Based Electrochemical Sensor for Detection of SARS-CoV-2 Antigen. *Biosens. Bioelectron.* **2021**, *178*, 113029. https://doi.org/10.1016/j.bios.2021.113029.

(10) Ayankojo, A. G.; Boroznjak, R.; Reut, J.; Öpik, A.; Syritski, V. Molecularly Imprinted Polymer Based Electrochemical Sensor for Quantitative Detection of SARS-CoV-2 Spike Protein. *Sens. Actuators B Chem.* **2022**, *353*, 131160. https://doi.org/10.1016/j.snb.2021.131160.

(11) Sharma, P. S.; Garcia-Cruz, A.; Cieplak, M.; Noworyta, K. R.; Kutner, W. 'Gate Effect' in Molecularly Imprinted Polymers: The Current State of Understanding. *Curr. Opin. Electrochem.* **2019**, *16*, 50–56. https://doi.org/10.1016/j.coelec.2019.04.020.

(12) Tsumoto, K.; Ejima, D.; Senczuk, A. M.; Kita, Y.; Arakawa, T. Effects of Salts on Protein–Surface Interactions: Applications for Column Chromatography. *J. Pharm. Sci.* **2007**, *96* (7), 1677–1690. https://doi.org/10.1002/jps.20821.

(13) Bard, A. J.; Faulkner, L. R. *Electrochemical Methods: Fundamentals and Applications*, 2nd ed.; Wiley: New York, 2001.

(14) Herres, D. *Father of electricity, William Gilbert*. https://www.testandmeasurementtips.com/7418/ (accessed 2022-03-18).

(15) Blom, J. *What is Electricity*. Sparkfun, Start Something. https://learn.sparkfun.com/tutorials/what-is-electricity/flowing-charges (accessed 2022-04-13).

(16) Herres, D. *The galvanic cell and Luigi Galvani*. https://www.testandmeasurementtips.com/the-galvanic-cell-and-luigi-galvani/ (accessed 2022-03-18).

(17) Flowers, P.; Robinson, W. R.; Langley, R.; Theopold, K. *Chemistry - 17.2 Galvanic Cells*; OpenStax: Houston, Texas, 2015.

(18) Harvey, D. *Voltammetric and Amperometric Methods*. ChemLibreTexts. https://chem.libretexts.org/@go/page/154799 (accessed 2022-04-26).

(19) *Mass Transport Mechanisms*. https://chem.libretexts.org/@go/page/61293 (accessed 2022-04-26).

(20) Fahmy Taha, M. H.; Ashraf, H.; Caesarendra, W. A Brief Description of Cyclic Voltammetry Transducer-Based Non-Enzymatic Glucose Biosensor Using Synthesized Graphene Electrodes. *Appl. Syst. Innov.* **2020**, *3* (3), 32. https://doi.org/10.3390/asi3030032.
(21) Wang, J.; John Wiley & Sons, L. *Analytical Electochemistry (Second Edition)*; Wiley-VCH, 2000.
(22) Bakirhan, N. K.; Kaya, S. I.; Ozkan, S. A. Chapter 2 - Basics of Electroanalytical Methods and Their Applications with Quantum Dot Sensors. In *Electroanalytical Applications of Quantum Dot-Based Biosensors*; Uslu, B., Ed.; Micro and Nano Technologies; Elsevier, 2021; pp 37–80. https://doi.org/10.1016/B978-0-12-821670-5.00011-7.
(23) Skoog, D. A.; West, D. M.; Holler, F. J. *Fundamentals of Analytical Chemistry*, 7th ed.; Saunders golden sunburst series; Saunders College Pub: Fort Worth, 1996.
(24) Physical Chemistry Laboratory in "Universitat De Valencia." Laboratory Session 2: Potentiometric and Voltammetric Study of the Ferricyanide/Ferrocyanide Redox Couple in Aqueous Solution of Potassium Chloride, 2019.
(25) Bioanalytical Systems, Inc. *Instruction Manual For Epsilon For Electrochemistry, Pulse Voltammetric Techniques*. https://www.basinc.com/manuals/EC_epsilon/Techniques/Pulse/pulse (accessed 2022-03-18).
(26) Ronkainen, N. J.; Halsall, H. B.; Heineman, W. R. Electrochemical Biosensors. *Chem. Soc. Rev.* **2010**, *39* (5), 1747–1763. https://doi.org/10.1039/B714449K.
(27) Heller, A.; Feldman, B. Electrochemical Glucose Sensors and Their Applications in Diabetes Management. *Chem. Rev.* **2008**, *108* (7), 2482–2505. https://doi.org/10.1021/cr068069y.
(28) Fatoyinbo, H. O.; Hughes, M. P. Biosensors. In *Encyclopedia of Nanotechnology*; Bhushan, B., Ed.; Springer Netherlands: Dordrecht, 2012; pp 329–345. https://doi.org/10.1007/978-90-481-9751-4_129.
(29) *Optical Biosensors - Interrogation methods*. Pyroistech. https://www.pyroistech.com/optical-biosensors/ (accessed 2022-04-13).
(30) Clark, L. C. Jr.; Lyons, C. Electrode Systems for Continuous Monitoring in Cardiovascular Surgery. Medical College of Alabama. 1962, pp 29–45.
(31) Suhito, I. R.; Koo, K.-M.; Kim, T.-H. Recent Advances in Electrochemical Sensors for the Detection of Biomolecules and Whole Cells. *Biomedicines* **2020**, *9* (1), 15. https://doi.org/10.3390/biomedicines9010015.
(32) Stradiotto, N. R.; Yamanaka, H.; Zanoni, M. V. B. Electrochemical Sensors: A Powerful Tool in Analytical Chemistry. *J. Braz. Chem. Soc.* **2003**, *14*, 159–173. https://doi.org/10.1590/S0103-50532003000200003.
(33) You, W.; Hui, X.; Jianming, Z.; Li, G. Electrochemical Sensors for Clinic Analysis. **2008**, 2043–2081.
(34) Moro, G.; De Wael, K.; Moretto, L. M. Challenges in the Electrochemical (Bio)Sensing of Nonelectroactive Food and Environmental Contaminants. *Curr. Opin. Electrochem.* **2019**, *16*, 57–65. https://doi.org/10.1016/j.coelec.2019.04.019.
(35) Ye, L.; Mosbach, K. Molecular Imprinting: Synthetic Materials As Substitutes for Biological Antibodies and Receptors†. *ACS Publ.* **2008**. https://doi.org/10.1021/cm703190w.
(36) BelBruno, J. J. Molecularly Imprinted Polymers. *Chem. Rev.* **2019**, *119* (1), 94–119. https://doi.org/10.1021/acs.chemrev.8b00171.
(37) Mujahid, A.; Dickert, F. L. 5 - Molecularly Imprinted Polymers: Principle, Design, and Enzyme-Like Catalysis. In *Molecularly Imprinted Catalysts*; Li, S., Cao, S., Piletsky, S. A., Turner, A. P. F., Eds.; Elsevier: Amsterdam, 2016; pp 79–101. https://doi.org/10.1016/B978-0-12-801301-4.00005-0.
(38) Boroznjak, R. *A Computational Approach for Rational Monomer Selection in Molecularly Imprinted Polymer Synthesis*; Thesis on natural and exact sciences; TUT Press: Tallinn, 2017.
(39) Tretjakov, A.; Syritski, V.; Reut, J.; Boroznjak, R.; Volobujeva, O.; Öpik, A. Surface Molecularly Imprinted Polydopamine Films for Recognition of Immunoglobulin G. *Microchim. Acta* **2013**, *180* (15), 1433–1442. https://doi.org/10.1007/s00604-013-1039-y.
(40) Kidakova, A.; Boroznjak, R.; Reut, J.; Öpik, A.; Saarma, M.; Syritski, V. Molecularly Imprinted Polymer-Based SAW Sensor for Label-Free Detection of Cerebral Dopamine Neurotrophic Factor

Protein. *Sens. Actuators B Chem.* **2020**, *308*, 127708. https://doi.org/10.1016/j.snb.2020.127708.
(41) Erdőssy, J.; Horváth, V.; Yarman, A.; Scheller, F. W.; Gyurcsányi, R. E. Electrosynthesized Molecularly Imprinted Polymers for Protein Recognition. *TrAC Trends Anal. Chem.* **2016**, *79*, 179–190. https://doi.org/10.1016/j.trac.2015.12.018.
(42) Mazzotta, E.; Di Giulio, T.; Malitesta, C. Electrochemical Sensing of Macromolecules Based on Molecularly Imprinted Polymers: Challenges, Successful Strategies, and Opportunities. *Anal. Bioanal. Chem.* **2022**. https://doi.org/10.1007/s00216-022-03981-0.
(43) Couto, R. A. S.; Costa, S. S.; Mounssef, B.; Pacheco, J. G.; Fernandes, E.; Carvalho, F.; Rodrigues, C. M. P.; Delerue-Matos, C.; Braga, A. A. C.; Moreira Gonçalves, L.; Quinaz, M. B. Electrochemical Sensing of Ecstasy with Electropolymerized Molecularly Imprinted Poly(o-Phenylenediamine) Polymer on the Surface of Disposable Screen-Printed Carbon Electrodes. *Sens. Actuators B Chem.* **2019**, *290*, 378–386. https://doi.org/10.1016/j.snb.2019.03.138.
(44) Bosserdt, M.; Gajovic-Eichelman, N.; Scheller, F. W. Modulation of Direct Electron Transfer of Cytochrome c by Use of a Molecularly Imprinted Thin Film. *Anal. Bioanal. Chem.* **2013**, *405* (20), 6437–6444. https://doi.org/10.1007/s00216-013-7009-8.
(45) Iskierko, Z.; Sharma, P. S.; Bartold, K.; Pietrzyk-Le, A.; Noworyta, K.; Kutner, W. Molecularly Imprinted Polymers for Separating and Sensing of Macromolecular Compounds and Microorganisms. *Biotechnol. Adv.* **2016**, *34* (1), 30–46. https://doi.org/10.1016/j.biotechadv.2015.12.002.
(46) Kříž, Z.; Klusák, J.; Krištofíková, Z.; Koča, J. How Ionic Strength Affects the Conformational Behavior of Human and Rat Beta Amyloids – A Computational Study. *PLOS ONE* **2013**, *8* (5), e62914. https://doi.org/10.1371/journal.pone.0062914.
(47) Usoltsev, D.; Sitnikova, V.; Kajava, A.; Uspenskaya, M. FTIR Spectroscopy Study of the Secondary Structure Changes in Human Serum Albumin and Trypsin under Neutral Salts. *Biomolecules* **2020**, *10* (4), 606. https://doi.org/10.3390/biom10040606.
(48) Dominy, B. N.; Perl, D.; Schmid, F. X.; Brooks, C. L. The Effects of Ionic Strength on Protein Stability: The Cold Shock Protein Family. *J. Mol. Biol.* **2002**, *319* (2), 541–554. https://doi.org/10.1016/S0022-2836(02)00259-0.
(49) Tsierkezos, N. G.; Ritter, U. Influence of Concentration of Supporting Electrolyte on Electrochemistry of Redox Systems on Multi-Walled Carbon Nanotubes. *Phys. Chem. Liq.* **2012**, *50* (5), 661–668. https://doi.org/10.1080/00319104.2012.663496.
(50) Fan, S. W.; George, R. A.; Haworth, N. L.; Feng, L. L.; Liu, J. Y.; Wouters, M. A. Conformational Changes in Redox Pairs of Protein Structures. *Protein Sci. Publ. Protein Soc.* **2009**, *18* (8), 1745–1765. https://doi.org/10.1002/pro.175.
(51) Konopka, S. J.; McDuffie, Bruce. Diffusion Coefficients of Ferri- and Ferrocyanide Ions in Aqueous Media, Using Twin-Electrode Thin-Layer Electrochemistry. *Anal. Chem.* **1970**, *42* (14), 1741–1746. https://doi.org/10.1021/ac50160a042.

# Appendix 1 - Settings for Cyclic Voltammetry measurements

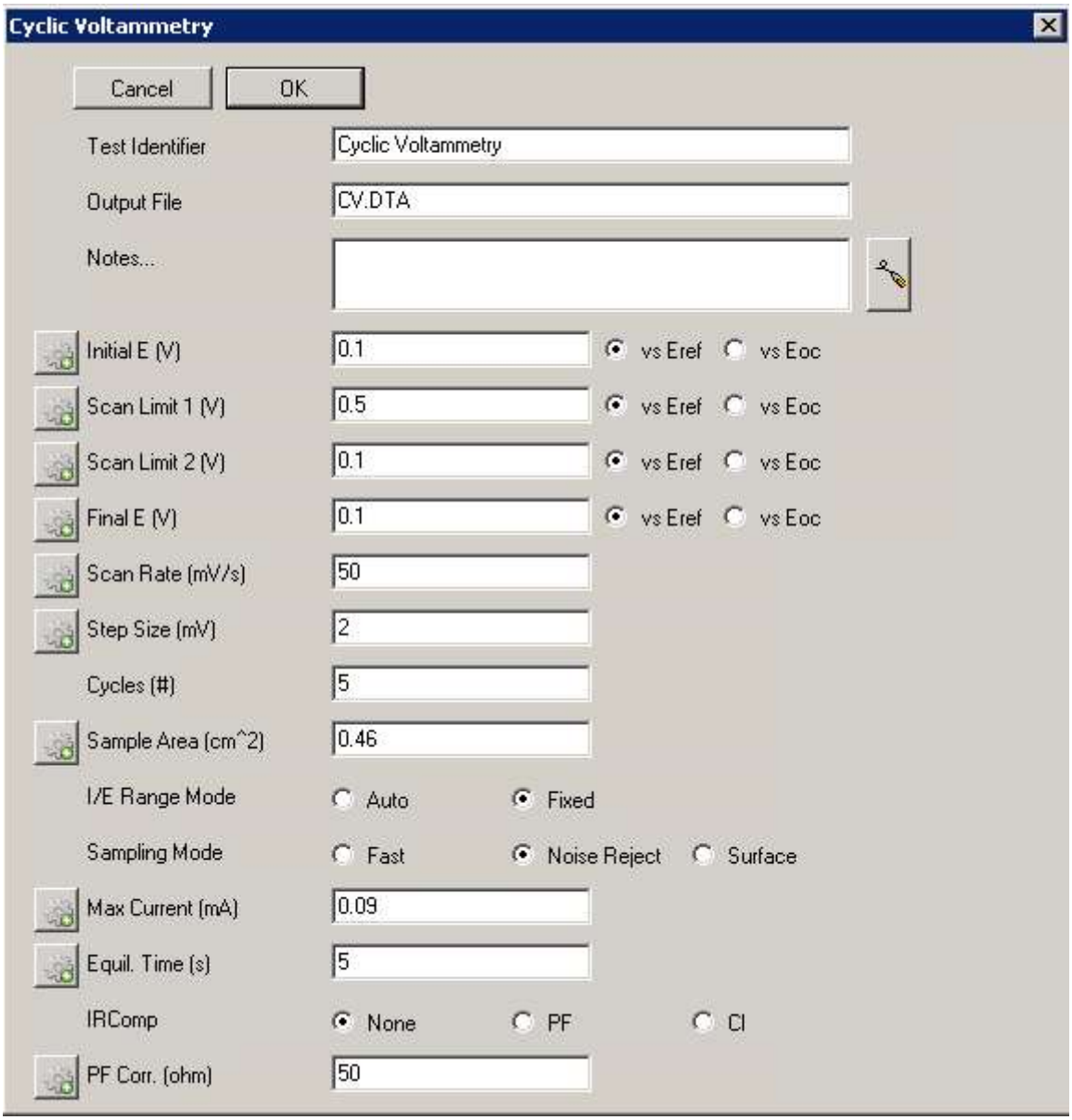

# Appendix 2 - Settings for Differential Pulse Voltammetry measurements

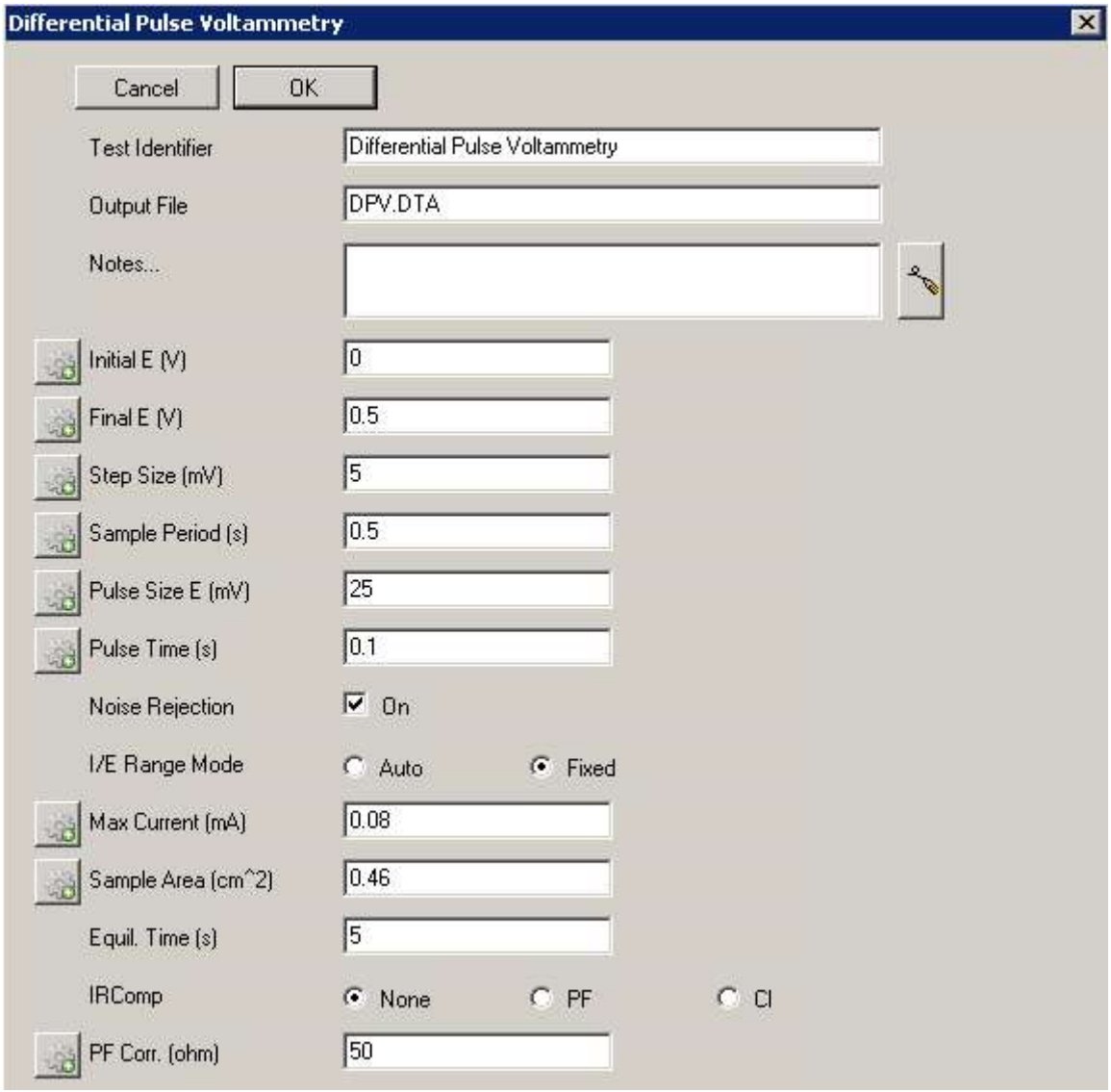

# Appendix 3 - BSA-MIP synthesis on WE

Figure A. CV of MIP-modified electrode formation on bare gold using (a) TPS and (b) UPS.

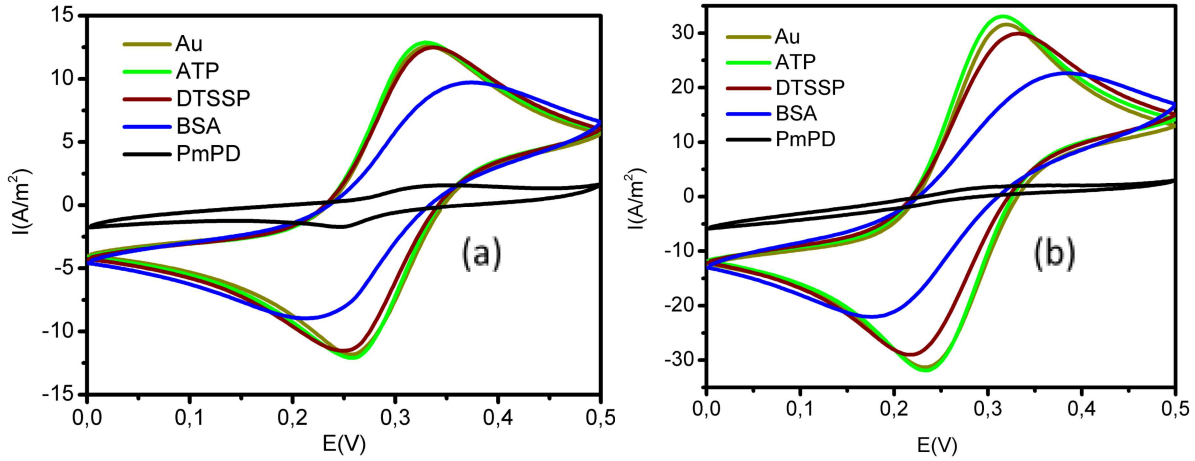


Figure B. CV of MIP-modified electrode washing out using (a) TPS and (b) UPS.

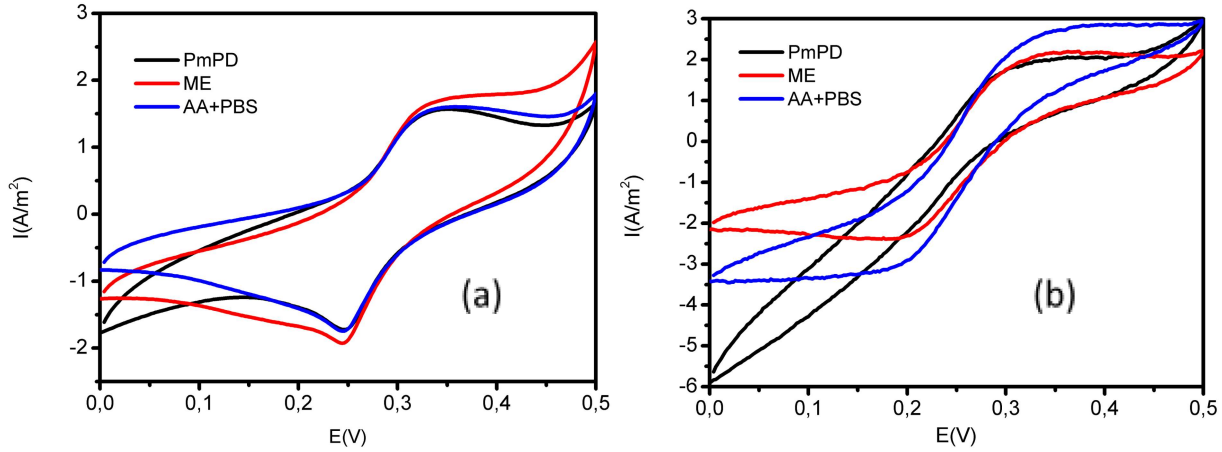

# Appendix 4 - DPV parameters of BSA adsorption study on bare gold

| BSA concentration, mg/mL | UPS | | TPS | |
|---|---|---|---|---|
| | $I_{max}$, $A/m^2$ | $I_n$ | $I_{max}$, $A/m^2$ | $I_n$ |
| 0 (PBS) | 24.38 | 0 | 11.24 | 0 |
| $10^{-9}$ | 21.23 | 0.13 | 11.02 | 0.02 |
| $10^{-8}$ | 16.32 | 0.33 | 10.73 | 0.05 |
| $10^{-7}$ | 11.40 | 0.53 | 10.47 | 0.07 |
| $10^{-6}$ | 8.66 | 0.64 | 10.05 | 0.12 |
| $10^{-5}$ | 6.95 | 0.71 | 9.44 | 0.16 |
| $10^{-4}$ | 5.44 | 0.77 | 8.17 | 0.27 |
| $10^{-3}$ | 3.88 | 0.84 | 5.76 | 0.49 |
| $10^{-2}$ | 2.51 | 0.90 | 4.05 | 0.64 |
| 1 | 1.67 | 0.93 | 2.84 | 0.75 |

## Appendix 5 - DPV parameters of BSA adsorption study on BSA-MIP-modified gold

| BSA concentration, mg/mL | UPS | | TPS | |
|---|---|---|---|---|
| | $I_{max}$, $A/m^2$ | $I_n$ | $I_{max}$, $A/m^2$ | $I_n$ |
| 0 (PBS) | 0.77 | - | 1.09 | - |
| $10^{-9}$ | 0.59 | 0.25 | 0.98 | 0.10 |
| $10^{-8}$ | 0.56 | 0.27 | 0.94 | 0.14 |
| $10^{-7}$ | 0.55 | 0.29 | 0.90 | 0.18 |
| $10^{-6}$ | 0.54 | 0.31 | 0.87 | 0.21 |
| $10^{-5}$ | 0.52 | 0.33 | 0.84 | 0.23 |
| $10^{-4}$ | 0.51 | 0.34 | 0.82 | 0.26 |
| $10^{-3}$ | 0.51 | 0.35 | 0.79 | 0.27 |
| $10^{-2}$ | 0.49 | 0.36 | 0.77 | 0.29 |
| 1 | 0.47 | 0.39 | 0.74 | 0.33 |

**Lihtlitsents lõputöö reprodutseerimiseks ja lõputöö üldsusele kättesaadavaks tegemiseks**[1]

Mina David Tsaregorodtsev,

1. Annan Tallinna Tehnikaülikoolile tasuta loa (lihtlitsentsi) enda loodud teose "The effect of redox probe solution composition on the response of the electrochemical biosensor", mille juhendaja on Jekaterina Reut,

1.1 reprodutseerimiseks lõputöö säilitamise ja elektroonse avaldamise eesmärgil, sh Tallinna Tehnikaülikooli raamatukogu digikogusse lisamise eesmärgil kuni autoriõiguse kehtivuse tähtaja lõppemiseni;

1.2 üldsusele kättesaadavaks tegemiseks Tallinna Tehnikaülikooli veebikeskkonna kaudu, sealhulgas Tallinna Tehnikaülikooli raamatukogu digikogu kaudu kuni autoriõiguse kehtivuse tähtaja lõppemiseni.

2. Olen teadlik, et käesoleva lihtlitsentsi punktis 1 nimetatud õigused jäävad alles ka autorile.

3. Kinnitan, et lihtlitsentsi andmisega ei rikuta teiste isikute intellektuaalomandi ega isikuandmete kaitse seadusest ning muudest õigusaktidest tulenevaid õigusi.

02.06.2022

[1] Lihtlitsents ei kehti juurdepääsupiirangu kehtivuse ajal vastavalt üliõpilase taotlusele lõputööle juurdepääsupiirangu kehtestamiseks, mis on allkirjastatud teaduskonna dekaani poolt, välja arvatud ülikooli õigus lõputööd reprodutseerida üksnes säilitamise eesmärgil. Kui lõputöö on loonud kaks või enam isikut oma ühise loomingulise tegevusega ning lõputöö kaas- või ühisautor(id) ei ole andnud lõputööd kaitsvale üliõpilasele kindlaksmääratud tähtajaks nõusolekut lõputöö reprodutseerimiseks ja avalikustamiseks vastavalt lihtlitsentsi punktidele 1.1. jq 1.2, siis lihtlitsents nimetatud tähtaja jooksul ei kehti.